Biomedicine & Pharmacotherapy 143 (2021) 112111

Contents lists available at ScienceDirect

Biomedicine & Pharmacotherapy

journal homepage: www.elsevier.com/locate/biopha

Rebound effects of NCX3 pharmacological inhibition: A novel strategy to accelerate myelin formation in oligodendrocytes

Mariarosaria Cammarota [a], Valeria de Rosa [a], Anna Pannaccione [a], Agnese Secondo [a], Valentina Tedeschi [a], Ilaria Piccialli [a], Ferdinando Fiorino [b], Beatrice Severino [b], Lucio Annunziato [c], Francesca Boscia [a,*]

[a] Division of Pharmacology, Department of Neuroscience, Reproductive Sciences and Dentistry, School of Medicine, Federico II University of Naples, Naples, Italy
[b] Department of Pharmacy, Federico II University of Naples, Naples, Italy
[c] IRCSS SDN, Naples, Italy

ARTICLE INFO

Keywords:
NCX3 exchanger
OPCs
Oligodendroglia
Myelin
BED blocker
Rebound effects

ABSTRACT

The Na^+/Ca^{2+} exchanger NCX3 is an important regulator of sodium and calcium homeostasis in oligodendrocyte lineage. To date, no information is available on the effects resulting from prolonged exposure to NCX3 blockers and subsequent drug washout in oligodendroglia. Here, we investigated, by means of biochemical, morphological and functional analyses, the pharmacological effects of the NCX3 inhibitor, the 5–amino-N-butyl-2–(4–ethoxyphenoxy)-benzamide hydrochloride (BED), on NCXs expression and activity, as well as intracellular $[Na^+]_i$ and $[Ca^{2+}]_i$ levels, during treatment and following drug washout both in human MO3.13 oligodendrocytes and rat primary oligodendrocyte precursor cells (OPCs). BED exposure antagonized NCX activity, induced OPCs proliferation and $[Na^+]_i$ accumulation. By contrast, 2 days of BED washout after 4 days of treatment significantly upregulated low molecular weight NCX3 proteins, reversed NCX activity, and increased intracellular $[Ca^{2+}]_i$. This BED-free effect was accompanied by an upregulation of NCX3 expression in oligodendrocyte processes and accelerated expression of myelin markers in rat primary oligodendrocytes. Collectively, our findings show that the pharmacological inhibition of the NCX3 exchanger with BED blocker maybe followed by a rebound increase in NCX3 expression and reversal activity that accelerate myelin sheet formation in oligodendrocytes. In addition, they indicate that a particular attention should be paid to the use of NCX inhibitors for possible rebound effects, and suggest that further studies will be necessary to investigate whether selective pharmacological modulation of NCX3 exchanger may be exploited to benefit demyelination and remyelination in demyelinating diseases.

1. Introduction

Progress in recent years has led to significant advances in understanding how $[Ca^{2+}]_i$ signaling network drive remyelination of demyelinated axons. Indeed, the importance of calcium signaling at the axo-myelinic synapse has been recently outlined by several findings providing evidence that calcium transients in developing oligodendrocytes, including those evoked by neuronal activity, drive myelin sheath elongation presumably controlling proteins regulating cytoskeletal growth and myelin assembly [1,2].

The Na^+/Ca^{2+} exchanger subtypes NCX1 and NCX3, by working either in the forward mode (Ca^{2+} extrusion) or in the reverse mode (Ca^{2+} entry) depending on the membrane potential and the transmembrane calcium and sodium gradients, participates in maintaining

Abbreviations: $[Ca^{+2}]_i$, intracellular calcium concentration; $[Na^+]_i$, intracellular sodium concentration; BED, 5–amino-N-butyl-2–(4–ethoxyphenoxy)benzamide hydrochloride; bFGF, basic fibroblast growth factor; BSA, bovine serum albumin; CAMKIIβ, calcium/calmodulin-dependent protein kinase IIβ; CNPase, 2',3'-Cyclic-nucleotide 3'-phosphodiesterase; D-Asp, D-Aspartate; DMSO, dimethyl sulfoxide solution; I_{NCX}, NCX currents; MBP, myelin basic protein; MS, multiple sclerosis; NCX, Na^+/Ca^{2+} exchanger; NCX3, Na^+/Ca^{2+} exchanger type 3; OPCs, oligodendrocyte precursor cells; PDGF-AA, platelet-derived growth factor-AA; RyRs, ryanodine receptors; wo, washout; α_2-NKA, sodium/potassium-transporting ATPase subunit alpha-2.

* Correspondence to: Division of Pharmacology, Department of Neuroscience, Reproductive Sciences and Dentistry, School of Medicine, Federico II University of Naples, Via Sergio Pansini 5, 80131 Naples, Italy.
E-mail address: boscia@unina.it (F. Boscia).

https://doi.org/10.1016/j.biopha.2021.112111
Received 8 April 2021; Received in revised form 20 August 2021; Accepted 23 August 2021
Available online 1 September 2021

intracellular $[Na^+]_i$ and $[Ca^{2+}]_i$ homeostasis in neurons and glial cells under demyelinating conditions [3–7]. Indeed, it has been proposed that dysfunctional NCX exchangers may contribute to detrimental calcium overload and axonal degeneration in white matter demyelinated axons [8–12]. This suggests that blocking NCX activity under certain demyelinating conditions might be axon-protective [13,14]. At variance, a number of studies in the last decade highlighted the protective function of NCX3 exchanger in brain ischemia and several neurodegenerative disease states, including demyelinating disorders [4,15–19], and suggest an important functional role of this exchanger for myelin synthesis in oligodendroglia [17,19–21]. Although more studies are required to better define the role of each NCX isoform in axon pathology during multiple sclerosis (MS) disease, current knowledge suggest that stimulating NCX3 activity may drive pro-differentiative effects in myelinating glia [17,22,23].

Currently, no positive modulators of NCX3 exchanger are still available, but many NCX blockers have been developed in the last decades. Given that the pharmacological effects of NCX blockers rely on what mode of NCX operation is more specifically blocked and which isoform is selectively inhibited, divergent effects on cell survival have been reported in physiological and pathophysiological conditions [24]. Furthermore, based on the observation that any change in NCX activity dynamically affect Na^+ and Ca^{2+} fluxes and that Na^+ and Ca^{2+} gradients tightly control the kinetics and directionality of NCX operation [4,25], more studies are required to understand the pharmacological effects of selective NCX3 blockers in oligodendroglia and neuronal cells under demyelinating conditions. These studies will be instrumental to develop and identify novel neurorepair strategies targeting NCX exchangers. Among NCX blockers, the 5–amino-N-butyl-2–(4-ethoxyphenoxy) benzamide hydrochloride (BED), a compound recently synthesized by our research group [26], is a potent NCX3 inhibitor that blocks both the *forward* and *reverse* mode of operation in the nanomolar range.

In the present study, by means of biochemical and confocal immunofluorescence studies, we first investigated the effects of the BED inhibitor on oligodendrocyte viability and NCXs expression at different time points after drug exposure and following drug-free washout both in human MO3.13 oligodendrocytes and rat primary oligodendrocyte precursor cells (OPCs). Then, by means of functional and morphological analysis, we investigated the effects of BED treatment and washout on sodium and calcium levels as well as on NCX activity and myelin synthesis in oligodendrocytes.

Collectively, our findings suggest that the pharmacological inhibition of NCX3 exchanger in oligodendrocytes with the BED blocker is followed by a rebound increase in NCX3 protein levels and reversal NCX activity that accelerated myelin sheet formation.

2. Material and methods

2.1. Animals

All animal experiments and animal handling and care were in accordance with the ARRIVE guidelines and the Guide for the Care and Use of Laboratory Animals (EU Directive 2010/63/EU), and the experimental protocol was approved by the Animal Care and Use Committee of "Federico II" University of Naples, Italy, and Ministry of Health, Italy (#515/2019-PR). Female Wistar rats (14-days timed pregnant) were obtained from Charles River Laboratories (Italy) and maintained at a constant temperature (22 −1 °C) on a 12-h light/dark cycle (lights on at 7 AM) with food and water ad libitum. The pregnant dams were allowed to deliver their pups naturally; 1–3 postpartum littermates were used for OPCs isolation. All efforts were made to minimize animal suffering and to reduce the number of animals used.

2.2. The human oligodendrocyte MO3.13 cell line and drug exposure

MO3.13 cells at passage 8 were maintained in Dulbecco's modified Eagle's medium (DMEM) supplemented with 10% fetal bovine serum (FBS), 100 U/ml penicillin, 10 lg/ml streptomycin, and 2 mmol/l glutamine (normal medium) [17]. During BED treatment and after its suspension, human MO3.13 cells were maintained in a serum-free chemically defined medium composed of DMEM supplemented with 500 μg/l insulin, 100 μg/ml human transferrin, 0.52 μg/l sodium selenite, 0.63 μg/ml progesterone, 16.2 μg/ml putrescine, 100 U/ml penicillin, 100 μg/ml streptomycin, 2 mM glutamine, 5 mg/ml N-acetyl-L-cysteine, and 10 μM D-biotin (OPC medium). 10–300 nM BED was incubated for 2, 4, or 6 days. Fresh drug was added to the cultures every 48 h in fresh medium. The calpain inhibitor, 300 nM calpeptin, was incubated at 1 day after BED washout for 15–17 h. Control cultures were kept in OPC medium.

2.3. Rat primary OPCs cultures and drug exposure

OPCs cultures were prepared as previously described [17]. OPCs were plated onto poly-D-lysine coated plates in OPC medium supplemented with 10 ng/ml recombinant human platelet-derived growth factor-AA (PDGF-AA) and 10 ng/ml basic fibroblast growth factor (bFGF) each day for 3–4 days to maintain the undifferentiated state at 37 °C in a humidified, 5% CO_2 incubator. BED was added to OPCs cultures the day after plating and kept in OPC medium supplemented with mitotic factors for 4 days. Fresh drug was added every 2 days. Control cultures were kept in OPC medium.

2.4. MTT assay

The MTT analyses were performed by incubating cells with (3- 4, 5-dimethylthiazol-2-yl)-2, 5-diphenyltetrazolium bromide (MTT, 0.5 mg/ml) at 37 °C in a 5% CO_2, 95% air atmosphere for 30 min. Then, the MTT solution was replaced with dimethyl sulfoxide solution (DMSO, 1 ml to each well), and the MTT absorbance was measured at 590 nm using a spectrophotometer (Eppendorf BioPhotometer).

2.5. Western blotting

Lysates from human MO3.13 progenitors and OPCs were separated on 8 or 14% polyacrylamide gel and electrophoretically transferred onto nitrocellulose membranes, as described [27,28]. Filters were probed with the indicated primary antibodies: rabbit polyclonal anti-NCX3 (1:500, Abcam), mouse monoclonal anti-NCX1 (Swant, 1:1000 dilution), rabbit polyclonal anti-NCX2 (Alpha Diagnostics International, 1:1000 dilution), rabbit polyclonal anti-sodium/potassium-transporting ATPase subunit alpha-2 (α_2-NKA, 1:1000, Proteintech), anti-β–actin (1:1000, Sigma, Italy), Proteins were visualized with peroxidase-conjugated secondary antibodies, using the enhanced chemiluminescence system (Amersham-Pharmacia Biosciences LTD, Uppsala, Sweden). Films were scanned and the signal ratio protein of interest/housekeeping protein was quantified densitometrically.

2.6. In vitro NCX3 silencing

Silencing of NCX3 in MO3.13 cells was performed by using the HiPerFect Transfection Kit (Qiagen, Milan, Italy), by using the following FlexiTube siRNAs for NCX3, Hs_Slc8A3(#8) 50-CACCACGCTCTTGCTTCCTAA-30, and a validated irrelevant AllStars siRNA as a negative control (siCtl), as previously described [17,22]. Following BED treatment for 4 days, cells were incubated with Opti-MEM (Invitrogen) supplemented with the RNAiFect Transfection Reagent (Qiagen) and 20 nM of the siRNA duplex for 6 h. Cells were incubated in BED-free OPC medium for 48 h before performing electrophysiological recordings.

2.7. Confocal immunofluorescence analysis

Confocal immunofluorescence procedures in cells were performed as previously described [29–31]. Cell cultures were fixed in 4% wt/vol paraformaldehyde in phosphate buffer for 30 min. After blocking with 3% BSA, cells were incubated with the following primary antibodies for 24 h. The primary antibodies used were the following: rabbit polyclonal anti-NCX3 (1:4000, Swant); rabbit polyclonal anti-α_2-NKA (1:1000, Proteintech); mouse monoclonal anti-CNPase (1:1000, Millipore), rat monoclonal anti-myelin basic protein (MBP, 1:1000, Merk), mouse monoclonal anti-calcium/calmodulin-dependent protein kinase IIβ (CAMKIIβ, 1:2000, Life technologies), mouse monoclonal anti-ki67 (1:500, eBioscience, Italy). Then, cells were incubated with corresponding fluorescence- labeled secondary antibodies (Alexa488- or Alexa594-conjugated anti-mouse or anti-rabbit IgGs). Dapi was used to stain nuclei. Images were observed using a Zeiss LSM 700 laser (Carl Zeiss) scanning confocal microscope. Single images were taken with an optical thickness of 0.7 μm and a resolution of 1024 × 1024. All staining and morphological analyses were blindly conducted.

2.7.1. Quantitative analysis

Images were processed and analyzed with the public domain Java-based image processing software ImageJ (National Institutes of Health, Bethesda, Maryland, USA).

A schematic diagram of oligodendrocyte lineage phenotypes, classified based on their morphology, the expression of the immature and mature oligodendrocytes markers used in this study, and phalloidin staining, is showed in the Supplemental Fig. S1.

The number of $NG2^+$ cells displaying no NCX3 immunoreactivity (NCX3-negative cells) and NCX3 immunoreactivity only in the soma (S) or both in the soma and proximal processes (S+P), as well as the number of $NG2^+$ cells displaying α_2-NKA immunoreactivity, Ki67 signal in the nucleus, and the number of double-labelled $NCX3^+/MBP^+$ cells was determined by manual counting at × 40 magnification. In NG2/NCX3 colocalization studies, all cells with bipolar or multipolar morphology showing a clearly visible punctate NCX3 labeling were counted. Quantification of CAMKIIβ and α_2-NKA fluorescence intensities were quantified in terms of pixel intensity by using the NIH image software, as described previously [17,22]. Briefly, digital images were taken with 63 × objective and identical laser power settings and exposure times were applied to all the photographs from each experimental set. Oligodendroglial cell morphology in vitro was evaluated with Alexa594–phalloidin (Thermo Fisher Scientific, Milan, Italy), as previously described [22,32]. Individual phalloidin-positive oligodendrocytes were scored according to their morphological complexity in four categories: (i) *bipolar/stellate,* defined as cells having from two to four processes; *multipolar*, including cells having more than four radially oriented processes, (ii) *arborized*, including cells with radially oriented arborization pattern containing intersections (iii) *partial ring,* including cells with arborized morphology but also containing ring-like regions; and (iv) *ring*, including oligodendrocytes with fully ring-like morphology. Quantification of relative cell surface area occupied by MBP protein was performed with ImageJ using the application: threshold from background, followed by manually defining the area, and finally measuring the area fraction above the threshold.

2.8. Microfluorimetric $[Ca^{2+}]_i$ and $[Na^+]_i$ measurements

Intracellular changes in $[Ca^{2+}]_i$ and $[Na^+]_i$ were measured by means of single-cell Fura-2 AM and sodium-binding benzofuran isophthalate (SBFI) video-imaging technique, in oligodendrocyte MO3.13 progenitors and rat primary OPCs plated on 10 μg/ml poly-D-lysine-coated glass coverslips, as previously described [33].

2.8.1. Fura-2 calcium imaging

Cells were incubated with 6 mM Fura-2 AM for 30 min at 37 °C in normal Krebs solution containing 5.5 mM KCl, 160 mM NaCl, 1.2 mM $MgCl_2$, 1.5 mM $CaCl_2$, 10 mM glucose, and 10 mM HEPES-NaOH (pH 7.4). Then, the coverslips were placed into a perfusion chamber (Medical System Co., Greenvale, NY, USA), mounted onto the stage of an inverted Zeiss Axiovert 200 microscope (Carl Zeiss, Milan, Italy), equipped with a FLUAR 40 × oil objective lens. The experiments were carried out with a digital imaging system composed of a MicroMax 512BFT cooled CCD camera (Princeton Instruments), LAMBDA10–2 filter wheeler (Sutter Instruments), and Meta-Morph/MetaFluor Imaging System software (Universal Imaging). Cells were alternatively illuminated at wavelengths of 340 and 380 nm by a Xenon lamp. The emitted light was passed through a 512 nm barrier filter. Fura-2 fluorescence intensity was measured every 3 s. Fura-2 ratiometric values were automatically converted by Meta-Morph/MetaFluor Imaging System software (Universal Imaging) to $[Ca^{2+}]_i$, by using a preloaded calibration curve obtained in preliminary experiments, as described [34].

Both sodium-free induced calcium response and intracellular Ca^{2+} transients after 100 μM D-Aspartate (D-Asp) stimulation were recorded in primary oligodendrocyte cultures by using the Meta-Morph/MetaFluor Imaging System software (Universal Imaging). $[Ca^{2+}]_i$ was analyzed within the traced rows at the cell soma and proximal processes, as indicated in Fig. 7B. For each cell, 3–4 proximal processes were recorded. The effect of D-Asp was quantified as Δ% of peak-basal values of $[Ca^{2+}]_i$. The mean value of the last 10 s of acquisition was considered the peak useful for the quantification.

2.8.2. SBFI sodium imaging

To load SBFI, coverslips plated with cells were placed in standard perfusion medium containing 10 μM SBFI-AM and 0.1% Pluronic F-127 in the presence of 5 mg/ml bovine serum albumin, and incubated for 120–180 min at 37 °C. Then, coverslips were placed in standard medium for 20 min to ensure de-esterification of the dye and then mounted in the chamber. Cells were excited alternately at 334 and 380 nm via a × 40 LD Achroplan objective, by using the same apparatus described above for Fura-2 experiments. The in vitro calibration of SBFI was accomplished by using the in situ procedure, according to Diarra et al. [35]. Specifically, SBFI ratios measured during the course of experiments were transformed into $[Na^+]_i$ values by a "one-point" procedure in which, at the end of an experiment, SBFI-loaded cells were exposed to a pH 7.3 medium containing 10 mM Na^+ and 4 μM gramicidin D.

2.9. Electrophysiology

NCX currents (I_{NCX}) in human MO3.13 oligodendrocytes were recorded by the patch-clamp technique in whole-cell configuration using the amplifier Axopatch200B and Digidata1322A interface (Molecular Devices), as previously described [15,36,37]. I_{NCX} were recorded starting from a holding potential of − 60 mV up to a short-step depolarization at + 60 mV (60 ms). A descending voltage ramp from + 60 mV to − 120 mV was applied. I_{NCX} recorded in the descending portion of the ramp (from +60 mV to −120 mV) were used to plot the current-voltage (I–V) relation curve. The I_{NCX} magnitude was measured at the end of + 60 mV (reverse mode) and at the end of − 120 mV (forward mode), respectively. The Ni^{2+}-insensitive component was subtracted from total currents to isolate I_{NCX}. The MO3.13 cells were perfused with the external Ringer's solution containing the following (in mM): 126 NaCl, 1.2 NaHPO4, 2.4 KCl, 2.4 CaCl2, 1.2 MgCl2, 10 glucose, and 18 NaHCO3, pH 7.4. Twenty millimolar tetraethylammonium (TEA), and 10 mM nimodipine were added to Ringer's solution to abolish potassium and calcium currents. The dialyzing pipette solution contained the following (in mM): 100 Cs-gluconate, 10 TEA, 20 NaCl, 1 Mg-ATP, 0.1 $CaCl_2$, $2MgCl_2$, 0.75 EGTA, and 10 HEPES, adjusted to pH 7.2 with CsOH. Possible changes in cell size occurring after specific treatments were calculated by monitoring the capacitance of each cell membrane, which is directly related to the membrane surface area and by expressing

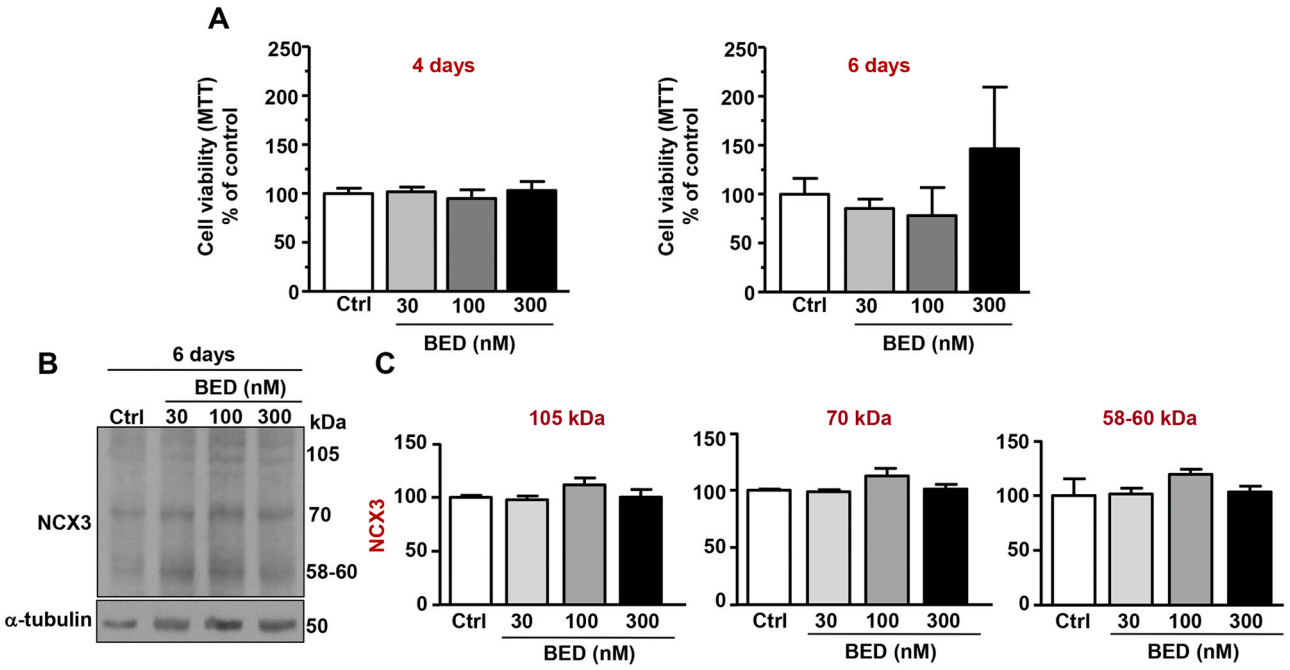

Fig. 1. Time and dose-depending effects of BED exposure on cell viability and NCX3 expression in human MO3.13 oligodendrocytes. A, Cell viability measured by MTT assay in M03.13 cells exposed to 10, 100, or 300 nM BED for 4 days (*left*) or 6 days (*right*). Data are expressed as percentage of control. The values represent the mean±S.E.M. (n = 3). **B**, Western blotting analysis of NCX3 protein levels from homogenates of MO3.13 oligodendrocytes cultured in the absence or in the presence of 30, 100, or 300 nM BED for 6 days; **C**, Densitometric analysis of the three major NCX3-specific enhanced chemiluminescence bands at ~105 kDa (*left*), 70 kDa (*middle*), and 58–60 kDa (*right*). Data were normalized on the basis of *α*-tubulin levels and expressed as percentage of control. The values represent the means±S.E.M (n = 3).

the current amplitude data as current densities (pA/pF). Capacitive currents were estimated from the decay of the capacitive transient induced by 5 mV depolarizing pulses from a holding potential of −80 mV and acquired at a sampling rate of 50 kHz. The capacitance of the membrane was calculated according to the following equation: Cm=tc·Io/DEm(1-I¥/Io), where Cm is membrane capacitance, tc is the time constant of the membrane capacitance, Io is the maximum capacitance current value, DEm is the amplitude of the voltage step, and I¥ is the amplitude of the steady-state current. I_{NCX} in the different experimental conditions were expressed as percentage of internal controls.

2.10. Statistical analysis

Statistical analysis was performed by using two-tailed Student's *t-test,* one-way ANOVA followed by Bonferroni or Tukey *post-hoc test* as indicated in the legends of figures. Analysis was done using the software GraphPad Prism 6. Values represent the mean ± SEM of at least three independent experiments. Differences were considered statistically significant at * $p < 0.05$.

3. Results

3.1. Drug washout following BED exposure upregulated NCX3 protein expression and stimulated reverse I_{NCX} in human MO3.13 oligodendrocytes

To test the effects of NCX3 blocking on cell viability, human MO3.13 oligodendrocyte cells were incubated with different concentrations of the NCX3 inhibitor 30–100–300 nM BED for 4 or 6 days. BED treatment did not significantly affected cell viability at any of the concentrations used or time points analysed, as revealed by MTT assay (Fig. 1A). Next, to evaluate whether prolonged BED exposure may influence NCX3 expression levels, human MO3.13 oligodendrocytes were incubated in the absence or in the presence of 30–100–300 nM BED for 6 days and cell lysates were analysed. In line with previous studies, the anti-NCX3 antibody revealed 3 main chemiluminescent bands in human MO3.13 lysates: a doublet of ~105 kDa corresponding to the full-length NCX3, a band of ~70 kDa and a cluster of bands of 58–60 kDa, referred as NCX3 calpain-cleaved fragments provided by exchanger activity [18] (Fig. 1B). Densitometric analysis of NCX3 immunoreactive bands showed that BED exposure for 2–4 days (data not shown) or 6 days (Fig. 1B-C) did not significantly affected NCX3 protein levels at neither of the concentration used (30–300 nM), if compared to untreated cultures.

Then, we tested the effects of BED washout on NCX3 protein distribution and expression following drug exposure in human MO3.13 oligodendrocytes. Confocal analysis performed with anti-NCX3 antibodies depicted a moderate NCX3 immunosignal in the cytosolic compartment either after 6 (Fig. 2A), 4 (Fig. 3A) or 2 days (data not shown) of BED exposure. One day after BED-free washout a pronounced plasma membrane NCX3 immunoreactivity was observed only in cells exposed to BED for 6 days (Fig. 2A, c). In MO3.13 oligodendrocytes exposed to BED for 6 or 4 days + 2 days after BED washout, a more intense NCX3 immunostaining was observed both in the cytosol and plasma membrane compartments if compared to untreated cells (Figs. 2A and 3A, respectively). Several intensely stained NCX3-positive cells with a rounded morphology were observed only in MO3.13 cultures exposed to 6 days BED + 2 days of washout (Fig. 2A, e). Nevertheless, the NCX3 inhibitor 100 nM BED did not significantly affected cell viability after 4 or 6 days of BED treatment + 2 days of washout, as revealed by MTT assay (Figs. 2D and 3D).

Western blot and quantitative densitometric analyses revealed that when cells were exposed to 100 nM BED for 6 days + 2 days of drug washout a significant upregulation of NCX3 bands at 58–60 kDa was observed (Fig. 2B-C). BED treatment for 4 days + 2 days washout significantly upregulated both the 70 kDa and 58–60 kDa NCX3 bands (Fig. 3B-C). Conversely, BED treatment for 2 days + 2 days washout did not alter NCX3 protein levels (data not shown). Moreover, analyses of

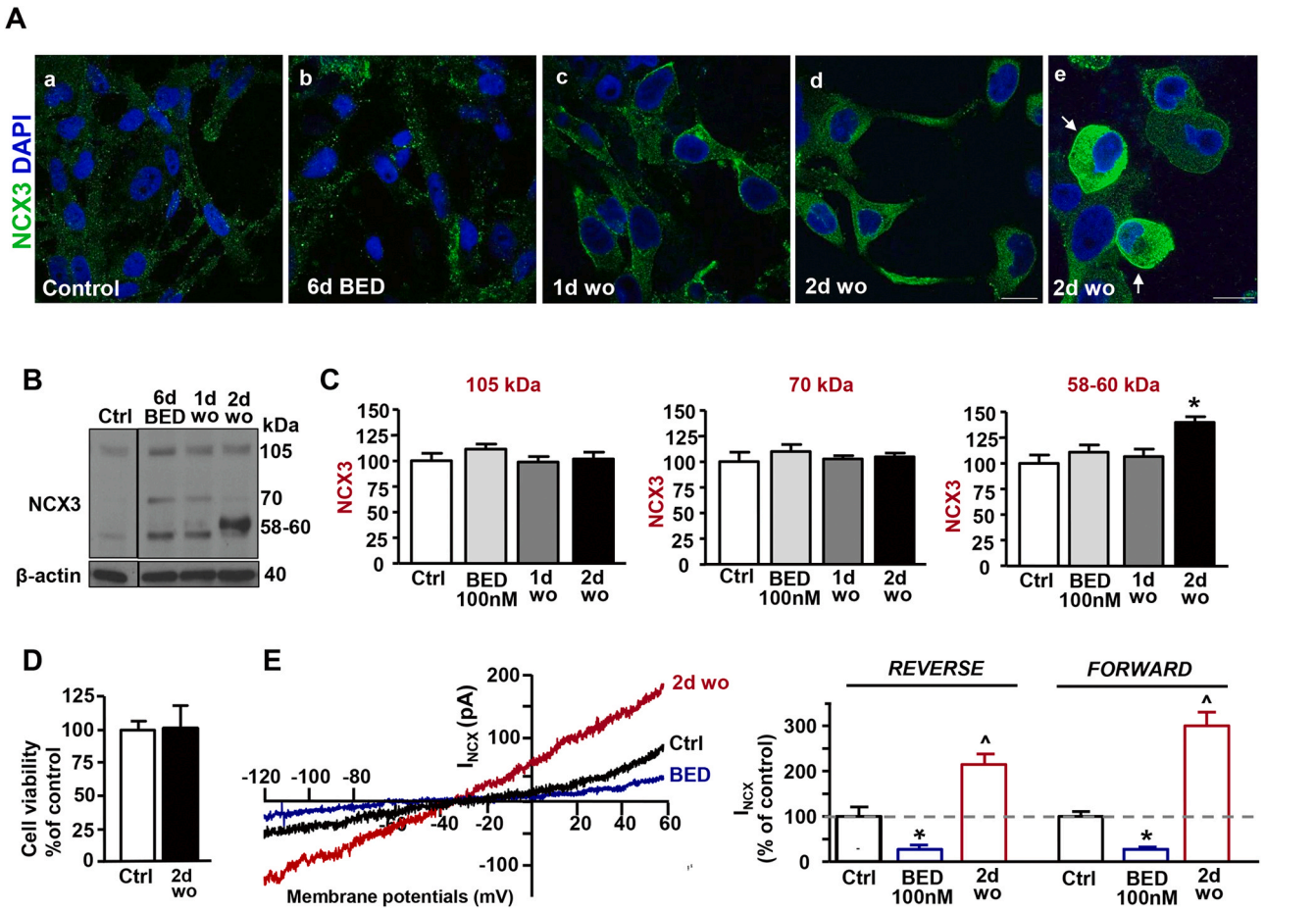

Fig. 2. Effect of 6-days BED treatment and washout on NCX3 expression and I_{NCX} in human MO3.13 oligodendrocytes. A, Representative confocal microscopic images showing NCX3 immunoreactivity in MO3.13 oligodendrocytes under control conditions (a), in the presence of 100 nM BED for 6 days (b), and after drug-free washout for 1 (c) or 2 days (d-e). Panel e shows a representative MO3.13 cells with rounded morphology displaying an intense NCX3 immunoreactivity within the soma and along plasma membrane (arrows). Scale bar: a-e: 20 μm. **B**, Western blotting analysis of NCX3 protein levels from homogenates of MO3.13 oligodendrocytes cultured under control conditions, in the presence of 100 nM BED for 6 days, and after drug-free washout for 1–2 days. **C**, Densitometric analysis of the three major NCX3-specific enhanced chemiluminescence bands of ~105 kDa (*left*), 70 kDa (*middle*), and 58–60 kDa (*right*). The data were normalized on the basis of *β*-actin levels and expressed as percentage of control. The values represent the means±S.E.M. (n = 3). *p < 0.05 versus control. **D**, Cell viability measured by MTT assay in untreated or M03.13-treated cells exposed to 100 nM BED for 6 days + 2 days after BED-washout. Data were expressed as percentage of control. The values represent the means±S.E.M. (n = 3). **E**, *left*. Representative I_{NCX}-superimposed traces recorded from MO3.13 oligodendrocytes under control conditions (black), in the presence of 100 nM BED for 6 days (blue), and 2 days after BED washout (red). **E**, *right,* I_{NCX} quantification is expressed as % of control in conditions, in the presence of 100 nM BED for 6 days and 2 days after BED washout. Each bar represents the mean±S.E.M. of the data obtained from 20 cells per group in three independent experimental sessions. *p < 0.05 versus control. (For interpretation of the references to colour in this figure legend, the reader is referred to the web version of this article.)

immunoreactive NCX3 bands revealed that BED treatment + washout did not significantly alter the ~105 kDa NCX3 band at any time point analysed (Figs. 2C and 3C).

Next, to investigate whether the increased NCX3 protein levels observed after BED treatment + drug washout was accompanied by an upregulation of NCX currents (I_{NCX}), we performed patch-clamp electrophysiology in MO3.13 oligodendrocytes. As expected, 100 nM BED treatment significantly reduced $I_{NCX,}$ both in the forward and reverse mode of operation, and either after 6 or 4 days of exposure (Figs. 2E and 3E, respectively). By contrast, I_{NCX}, recorded after 2 days of BED washout, significantly increased in cells exposed to 100 nM BED for 4 or 6 days. Interestingly, a selective enhancement of reverse NCX operational mode was recorded in MO3.13 oligodendrocytes exposed to BED for 4 days + 2 days of washout, while both the forward and reverse I_{NCX} increased in cells exposed to BED for 6 days + 2 days of washout (Fig. 2E). Dose-dependent electrophysiological responses showed that 30 nM BED was less effective to block I_{NCX} after 4 days of treatment, while it has no significant effect on I_{NCX} currents after drug washout. Conversely, 10 nM BED was ineffective to inhibit I_{NCX} during drug treatment or enhance I_{NCX} and NCX3 protein levels (data not shown) after drug washout (Fig. 3E).

Then, we evaluated the expression levels of NCX1 and NCX2 exchangers in response to 4- and 6-days 100 nM BED treatment and subsequent drug-free washout (Fig. 4). To this aim, filters were stripped and probed with anti-NCX1 and anti-NCX2 antibodies. Densitometric analysis of NCX1 major bands revealed that NCX1 protein levels were significantly upregulated by BED treatment after both 4 or 6 days. During BED-free washout NCX1 levels remained significantly higher in the 6-days protocol, while they returned to basal levels in the 4-days protocol (Fig. 4A-B). The 102 kDa band of NCX2 was not altered by BED treatment neither after 4 or 6 days. During BED-free washout NCX2 protein levels significantly increased after 2 days in the 6-days protocol, while they were only transiently upregulated after one day in the 4-days protocol (Fig. 4C-D). These results suggest that BED suspension after 4 days of exposure selectively enhanced reverse I_{NCX} activity and predominantly affected NCX3 levels 2 days after drug washout.

Finally, to further verify the involvement of NCX3 in BED-induced pharmacological effects, we silenced ncx3 gene in MO3.13 cells after 4

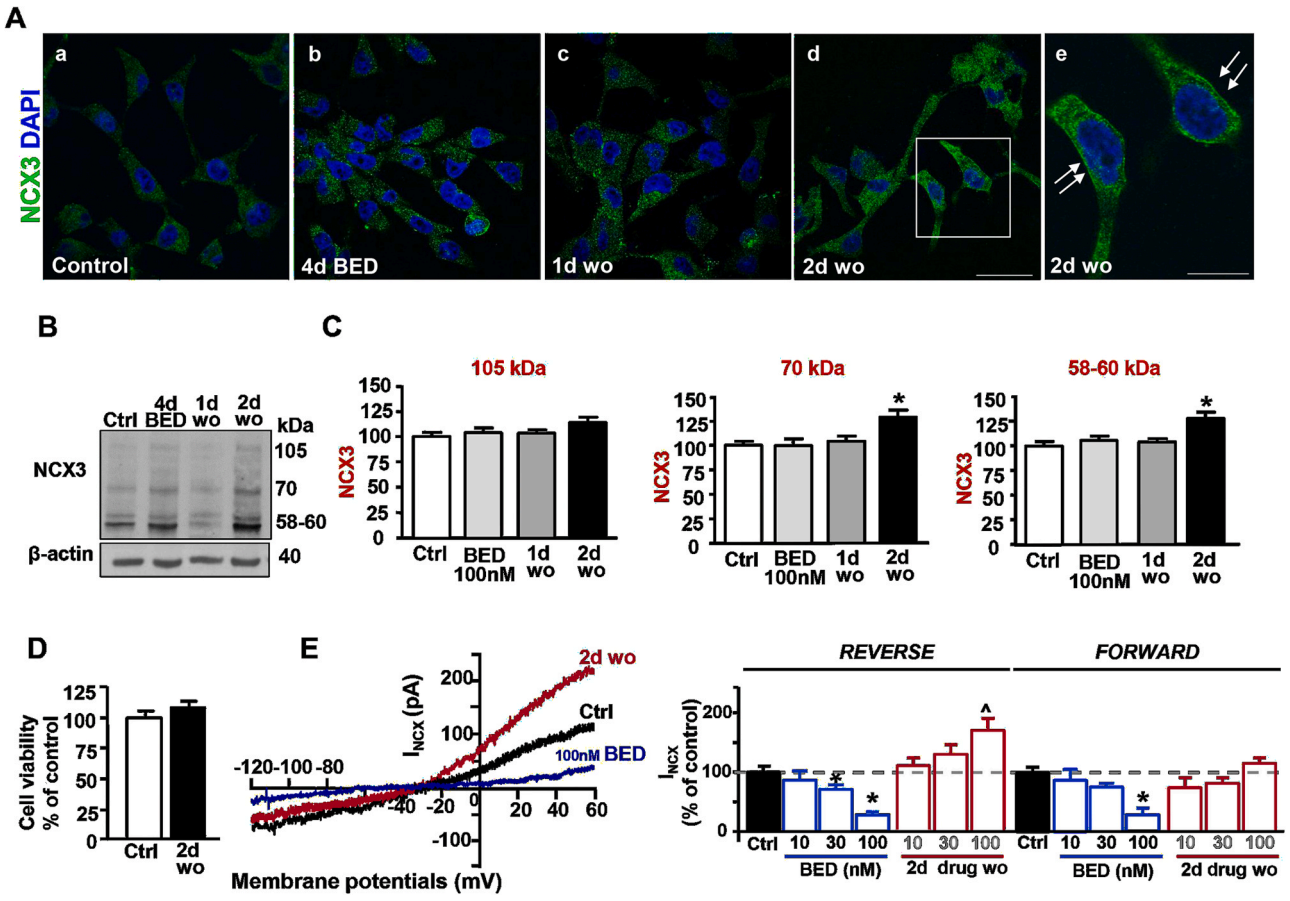

Fig. 3. Effect of 4-days BED treatment and washout on NCX3 expression and I_{NCX} in human MO3.13 oligodendrocytes. A, Representative confocal microscopic images showing NCX3 immunoreactivity in MO3.13 oligodendrocytes cultures under control conditions (a), in the presence of 100 nM BED for 4 days (b) and after drug-free washout for 1 (c) or 2 days (d-e). Panel e shows higher magnification image of the frame depicted in panel d. Arrows point to NCX3 immunoreactivity along cell plasma membrane. Scale bars in a-d: 50 μm; in e: 20 μm **B**, Western blotting analysis of NCX3 protein levels from homogenates of MO3.13 oligodendrocytes cultured under control conditions, in the presence of 100 nM BED for 4 days, and after drug-free washout for 1–2 days. **C**, Densitometric analysis of the three major NCX3-specific enhanced chemiluminescence bands of ~105 kDa (*left*), 70 kDa (*middle*), 58–60 kDa (*right*). The data were normalized on the basis of *β*-actin levels and expressed as percentage of control. The values represent the means±S.E.M. (n = 3). *p < 0.05 versus control. **D**, Cell viability measured by MTT assay in untreated or M03.13 cells exposed to 100 nM BED for 4 days + 2 days after BED-washout. Data were expressed as percentage of control. The values represent the means±S.E.M. (n = 3). **E**, *left.* Representative I_{NCX}-superimposed traces recorded from MO3.13 cells under control conditions (black), in the presence of 100 nM BED for 4 days (blue), and 2 days after BED washout (red). **E**, *right,* I_{NCX} quantification is expressed as % of control in control conditions, in the presence of 30–100 nM BED for 4 days and after 2 days of BED washout. Each bar represents the mean±S.E.M. of the data obtained from 20 cells per group in three independent experimental sessions. *p < 0.05 versus control. (For interpretation of the references to colour in this figure legend, the reader is referred to the web version of this article.)

days of BED treatment. Then, cells were kept in BED-free OPC medium for 48 h before performing electrophysiological analyses. As shown in Fig. 4E-F, silencing ncx3 gene during drug washout significantly prevented the upregulation reverse I_{NCX} activity. These results suggest that NCX3 significantly contributed to the reverse I_{NCX} activity recorded after 4 days of BED treatment + 2 days of BED-free washout.

3.2. *BED exposure induced $[Na^+]_i$ accumulation, and modulate α_2-NKA protein expression and $[Ca^{+2}]_i$ levels after drug washout in human MO3.13 oligodendrocytes*

Next, considering that $[Na^+]_i$ is the main regulator of exchange mode and activity of NCX [4,6], we speculated that the NCX3 inhibitor BED would partly occlude Na^+ extrusion and may induce $[Na^+]_i$ accumulation during prolonged exposure, consequently driving Ca^{2+} influx after drug washout. To test this hypothesis, by means of SBFI- and Fura-2 video-imaging, we first recorded intracellular $[Na^+]_i$ at 4 days after BED exposure, and then intracellular $[Ca^{2+}]_i$ after BED washout in human MO3.13 oligodendrocytes.

As shown, $[Na^+]_i$ levels significantly increased in MO3.13 cells exposed to 100 nM BED for 4 days if compared to untreated cells (Fig. 5A). Fura-2 video imaging showed that 3 h after BED washout a significant $[Ca^{2+}]_i$ rise was recorded in cultures exposed to 100 nM BED for 4 days if compared to untreated cells or BED-treated cells (Fig. 5B). The reverse NCX3 inhibitor, 100 nM YM-24476 [38], applied 2,5 h after BED washout, significantly prevented $[Ca^{2+}]_i$ rise in MO3.13 cells (Fig. 5B), thus suggesting that NCX3 activity contributes to BED washout-induced calcium increase.

Previous studies showed that a sustained increase in $[Ca^{2+}]_i$ may generate calpain-cleaved forms of NCX3 [39], that may lead to increased functional activity of the antiporter in reverse the mode of operation [18] or exchanger inactivation [39]. Hence, we investigated whether the increased NCX3 protein levels observed during BED washout in MO3.13 cells might be attributed to the exchanger cleavage mediated by calpains. To this aim, MO3.13 cultures were first incubated with BED for 4 days, and then with the calpain inhibitor, calpeptin, during drug washout. Western blots analysis showed that 300 nM calpeptin significantly prevented the upregulation of both 70 kDa and 58–60 kDa NCX3 bands if compared to untreated cultures (Fig. 5C-D), thus suggesting that the upregulation of NCX3 minor bands is associated with increased fragmentation of NCX3 exchanger mediated by a calcium-dependent activation of calpains.

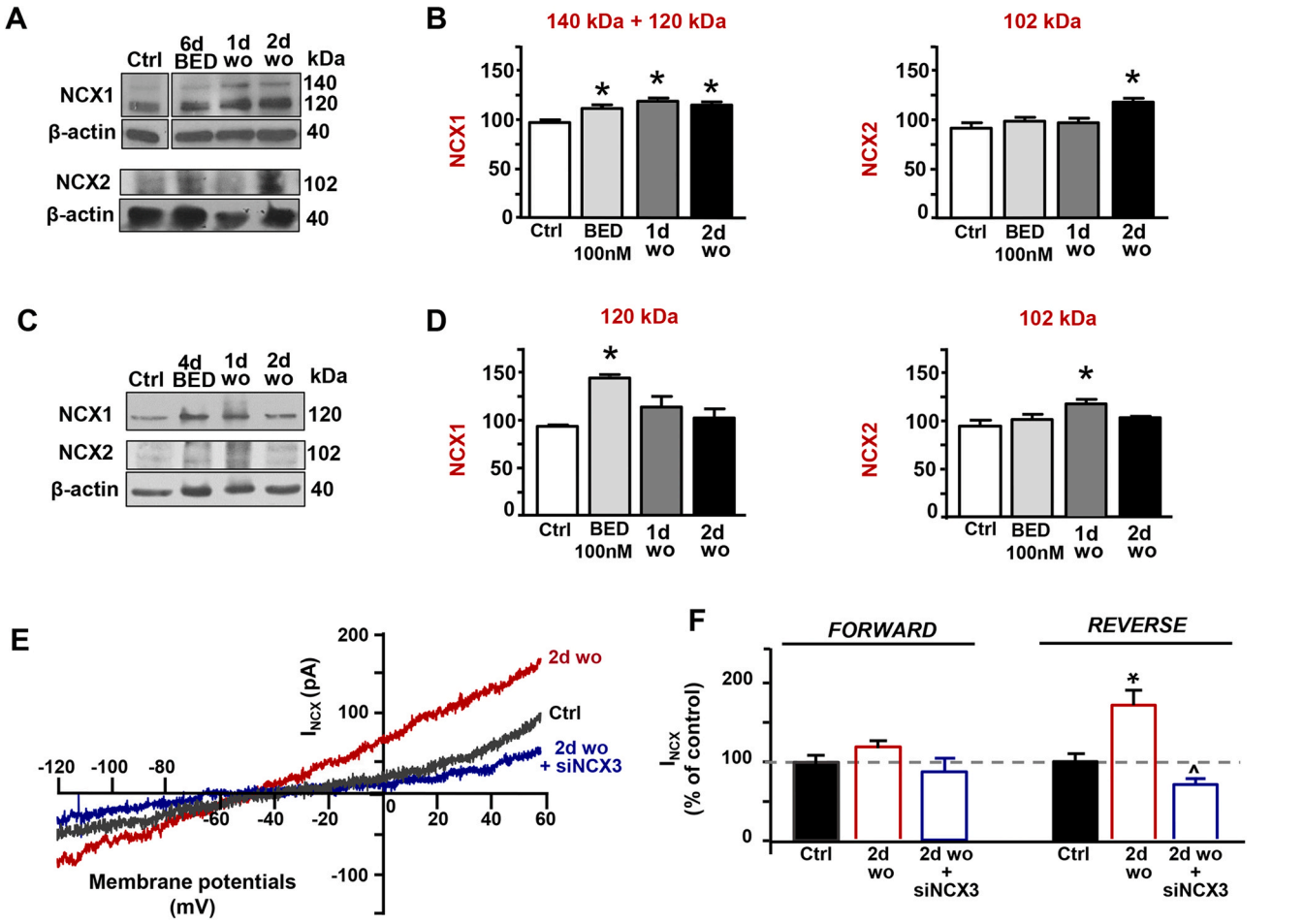

Fig. 4. Effect of BED treatment on NCX1 and NCX2 protein levels and of *ncx3* gene silencing on I_{NCX} in human MO3.13 oligodendrocytes. A-B, Western blot and densitometric analysis of NCX1 and NCX2 protein levels from homogenates of MO3.13 oligodendrocytes cultured under control conditions, in the presence of 100 nM BED for 6 days, and after drug-free washout for 1–2 days. The filter showed in Fig. 2B was stripped and blotted with anti-NCX1 antibody. **C-D**, Western blot and densitometric analysis of NCX1 and NCX2 protein levels from homogenates of MO3.13 oligodendrocytes cultured under control conditions, in the presence of 100 nM BED for 4 days, and after drug-free washout for 1–2 days. The filter showed in Fig. 5E was stripped and blotted with anti-NCX1 or anti-NCX2 antibodies. The values represent the means±S.E.M. (n = 3). *p < 0.05 versus control. **E**, Representative I_{NCX}-superimposed traces recorded from MO3.13 cells days after 4 days of 100 nM BED treatment + 2 days of BED washout under control conditions (black) and in absence (red) or in presence of siNCX3 (blue). **F**, I_{NCX} quantification is expressed as % of control. Each bar represents the mean±S.E.M. of the data obtained from 20 cells per group in three independent experimental sessions. *p < 0.05 versus control. (For interpretation of the references to colour in this figure legend, the reader is referred to the web version of this article.)

Then, based on the observation that the Na^+/K^+-ATPase (NKA), a major regulator of $[Na^+]_i$, and cell volume, is functionally coupled to NCX [40], and that the α_2-NKA isoform can modulate NCX-mediated Ca^{2+} influx in oligodendrocytes [21], we investigated the effects of BED exposure and washout on α_2-NKA protein levels. Densitometric analysis of Western blot experiments revealed that α_2-NKA protein levels remained unchanged after 4 days of BED exposure if compared to untreated cells, significantly decreased at 1 day of BED washout, and subsequently increased over the basal levels at 2 days of BED washout (Fig. 5E). Conversely, the α_2-NKA protein levels remained unchanged when human MO3.13 oligodendrocytes were exposed to BED for 2 days + 1 or 2 days of drug washout (Fig. 5F).

Based on recent findings showing that silencing α_2-NKA expression in oligodendrocytes not only stimulated NCX-mediated $[Ca^{2+}]_i$ rise but also boosted myelin marker expression, we explored the localization of the myelin marker CNPase in human MO3.13 oligodendrocytes during BED washout. Confocal double-labeling experiments and line profiling the CNPase (red) and NCX3 (green) fluorescence intensities showed an enhanced coexpression of NCX3 and CNPase immunoreactivities along plasma membrane domains of cell exposed to BED for 4 days + 2 days of drug washout (Fig. 5G).

3.3. Drug washout following BED exposure reduced OPCs proliferation and upregulated NCX3 expression and I_{NCX} activity in rat primary OPCs

To explore the pharmacological actions of BED exposure in rat primary OPCs, we first analysed the effects of 4 days BED exposure + drug-free washout on OPCs proliferation and on calcium/calmodulin-dependent kinase type IIβ (CaMKIIβ) expression, a critical component of the molecular mechanism regulating oligodendrocyte maturation [41,42] Based on the findings showing that blocking NCX activity prevented OPCs differentiation [17,20,22], we exposed OPCs in the presence of BED for 4 days during the proliferation stage, and then analyzed the effects on OPCs development after drug washout.

Quantitative confocal immunofluorescence analysis revealed that the number of $NG2^+$ cells coexpressing the nuclear proliferation marker Ki67 was significantly higher in cultures exposed to 100 nM BED for 2 days if compared to untreated cultures (Fig. 6A). After 4 days of BED treatment, the number of double-labelled $NG2^+/Ki67^+$ OPCs significantly increased in the control group, while no difference was observed among control and BED-treated cultures (Fig. 6A). One day after BED washout, the number of double-labelled $NG2^+/Ki67^+$ cells significantly decreased in BED-treated if compared to untreated cultures (Fig. 6A). In

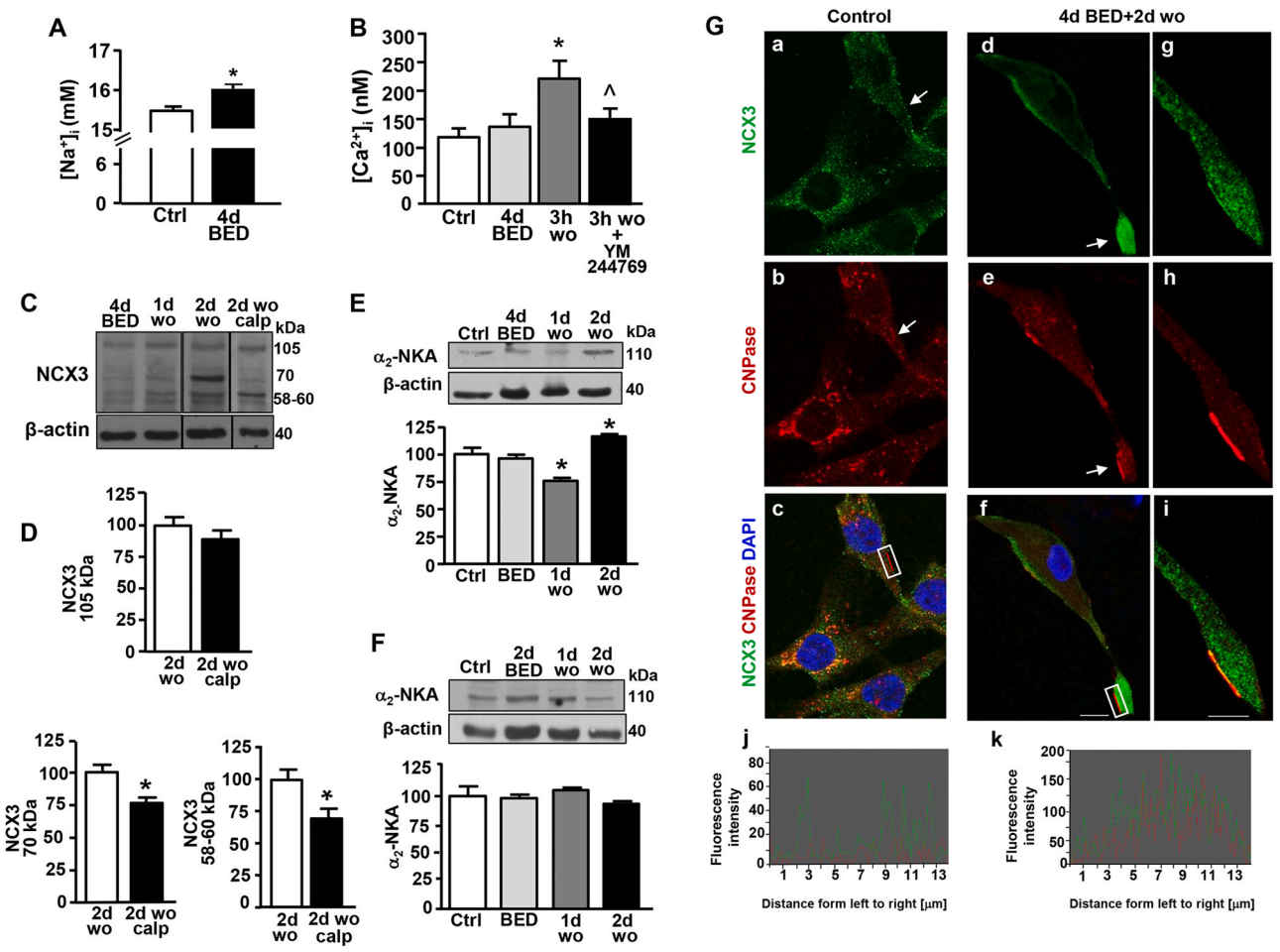

Fig. 5. Effects of 4-days BED treatment and washout on [Na^+] and [Ca^{2+}] levels, α 2-NKA and CNPase expression in human MO3.13 oligodendrocytes. A, Quantification of $[Na^+]_i$ detected with SBFI in MO3.13 oligodendrocytes under control conditions, and exposed to 100 nM BED for 4 days. Each bar represents the mean±S.E.M. of the data obtained from 30 cells per group in three independent experimental sessions. *p < 0.05 versus control. **B**, Quantification of $[Ca^{2+}]_i$ recorded with Fura-2 in MO3.13 cells under control conditions, after 100 nM BED for 4 days, and after 3 h of BED washout (3 h wo), in absence or in the presence of the NCX3 inhibitor 100 nM YM-24476. Each bar represents the mean±S.E.M. of the data obtained from 30 cells per group in three independent experimental sessions. *p < 0.05 versus control. and BED 4 days; ^p < 0.05 versus 3 h wo. **C**, Western blotting analysis of NCX3 protein levels from homogenates of MO3.13 oligodendrocytes cultured in the presence of 100 nM BED for 4 days, and after drug-free washout for 1–2 days, in the absence or in the presence of 300 nM calpeptin. **D**, Densitometric analysis of the three major NCX3-specific enhanced chemiluminescence bands of ~105 kDa, 70 kDa, 58–60 kDa. The data were normalized on the basis of β-actin levels and expressed as percentage of 2-days-washout. The values represent the means±S.E.M ($n = 3$). * $p < 0.05$ versus control. **E-F**, Western blotting and densitometric analysis of α_2-NKA protein levels from homogenates of MO3.13 oligodendrocytes cultured under control conditions, in the presence of 100 nM BED for 4 days (E) or 2 days (F) and after 1 or 2 days of drug-washout. The data were normalized on the basis of β-actin levels and expressed as percentage of control. The values represent the means±S.E.M. ($n = 4$). **G**, Confocal microscopic images displaying NCX3 (green) and CNPase (red) immunoreactivities in untreated (a-c) and MO3.13 oligodendrocytes treated with BED for 4 days + 2 days of drug-free-washout (d-i). Arrows in panels d-f point to the intense NCX3 and CNPase immunolabeling along plasma membrane. *j-k*, line profiling of NCX3 (green) and CNPase (red) fluorescence intensities along the line selected on the plasma membrane of both control (c) and BED-treated cell (f). Scale bars: a- f: 20 μm; g-i: 10 μm. (For interpretation of the references to colour in this figure legend, the reader is referred to the web version of this article.)

addition, one day after BED washout, $NG2^+$ cells displayed a significant upregulation of CAMKIIβ fluorescence intensity if compared to untreated OPCs (Fig. 6B). Quantitative confocal studies showed that the α_2-NKA immunofluorescence intensity in oligodendrocyte $NG2^+$ precursors was globally and significantly reduced 1 day after BED washout if compared to untreated cultures (Fig. 6C). Quantitative analysis showed that the number of double-labelled $NG2^+/\alpha_2$-NKA^+ cells with bipolar morphology was significantly reduced if compared to untreated cells (Fig. 6C, h). Conversely, a significant number of $NG2^+/\alpha_2$-NKA^+ cells with multipolar morphology was detected, suggesting that the α_2-NKA immunoreactivity is re-established in cells progressing to a more mature phenotype (Fig. 6C, h).

Next, we investigated the effects of BED exposure + drug-free washout on NCX3 expression and activity in primary OPCs cultures. Confocal double immunofluorescence analysis showed that the number of $NG2^+$ cells coexpressing NCX3 was significantly higher in OPCs exposed to BED for 4 days if compared to untreated cells. In undifferentiated OPCs, NCX3 immunoreactivity was moderately detected in the somatic compartment (Fig. 7A). Conversely, 2 days after BED washout, a significant increase in the number of multipolar $NG2^+$ cells displaying a punctuated NCX3 immunoreactivity both in the soma and along processes was observed, if compared to untreated cultures (Fig. 7A). In line, an upregulated chemiluminescence signal of NCX3 immunoreactive bands was revealed by Western blot analysis performed on OPCs lysates from cultures exposed to BED for 4 days + 2 days washout (Fig. 7B). Furthermore, NCX activity, recorded by Fura-2-video imaging at 2 days after BED washout, significantly increased both in oligodendrocyte soma and processes if compared to untreated cultures (Fig. 7C).

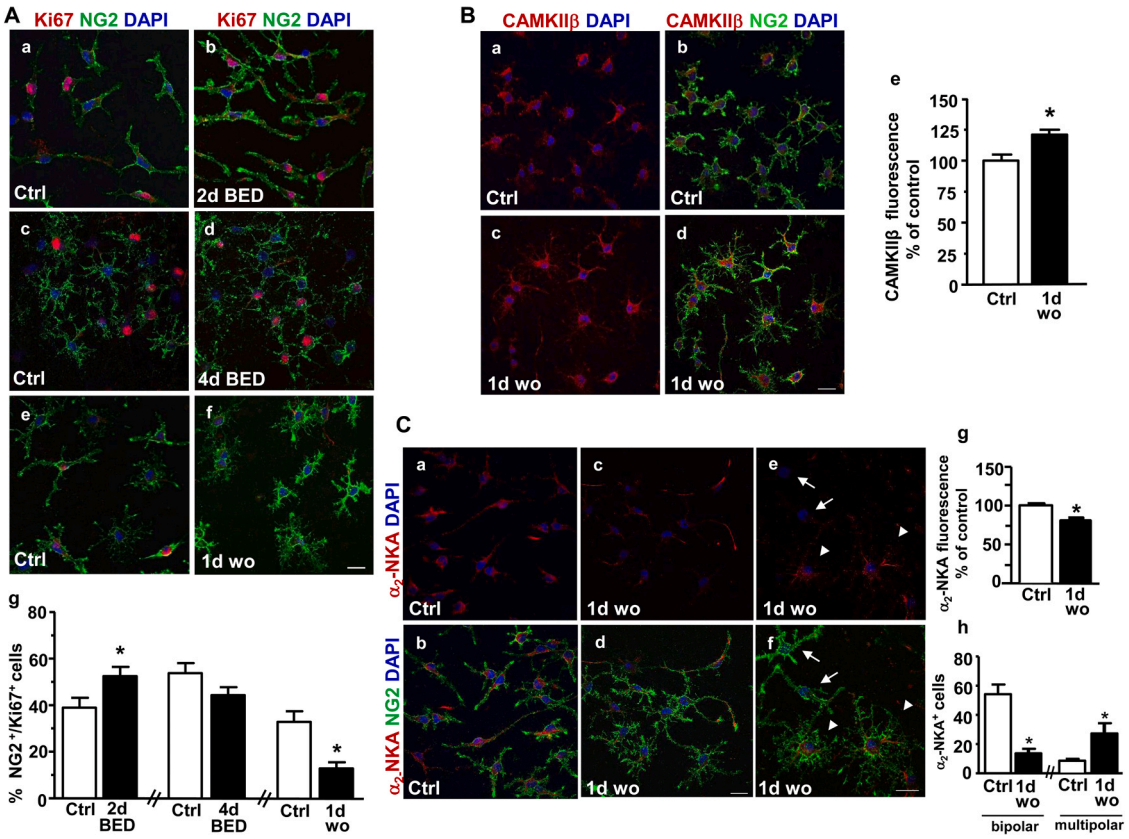

Fig. 6. Effects of 4-days BED treatment and washout on Ki67, CAMKIIβ, and α_2-NKA expression in rat primary OPCs. A, Representative confocal double immunofluorescence images (a-l) and quantitative analysis (g) of the number of $NG2^+$ cells (green) coexpressing the nuclear proliferation marker Ki67 (red) in rat primary OPCs under control conditions, after 2 or 4 days of BED treatment (a-b and c-d, respectively), and after 4 days of BED treatment + 1 day of drug-free-washout (e-f). Nuclei were counterstained with dapi (blue). Scale bars in a–f: 20 μm. **B,** Confocal double immunofluorescence images displaying the distribution of CAMKIIβ immunosignal (red) and NG2 (green) in rat primary OPCs under control conditions (a-b) and after 4 days of BED treatment + 1 day of drug-washout (c-d). e; quantitative analysis of CAMKIIβ fluorescence intensity in rat primary OPCs under control conditions and after 4 days of BED treatment + 1 day of drug-washout. Nuclei were counterstained with dapi (blue). Data were normalized to the total number $NG2^+$ cells. The values represent the means±S.E.M. ($n = 3$). * $p < 0.05$ versus control. Scale bars: a–d: 20 μm. **C**, Representative confocal images displaying the distribution of α_2-NKA (red) and NG2 (green) immunosignals in rat primary OPCs cultured under control conditions (a-b) and after 4 days of BED treatment + 1 day of drug-washout (c-f). Arrows in e-f point to bipolar $NG2^+$ cells showing a negligible α_2-NKA immunosignal; arrowheads in e-f point to multipolar $NG2^+$ cells displaying an α_2-NKA immunosignal along cell processes. Nuclei were counterstained with dapi (blue). g; quantitative analysis of α_2-NKA fluorescence intensity in rat primary OPCs under control conditions and after 4 days of BED treatment + 1 day of drug-washout. h, quantitative analysis of the number of bipolar and multipolar oligodendrocytes displaying α_2-NKA immunoreactivity after 1 day of BED-free washout. Data were normalized on to the total number of $NG2^+$ cells. The values represent the means±S.E.M. ($n = 3$). * $p < 0.05$ versus control. Scale bars: a–f: 20 μm. (For interpretation of the references to colour in this figure legend, the reader is referred to the web version of this article.)

3.4. Drug washout following BED exposure enhanced D-Aspartate-induced calcium response and accelerated myelin sheet formation in rat primary oligodendrocytes

We recently showed that D-Aspartate (D-Asp) exposure evoked a calcium response in OPCs that involve the activation of AMPA and NMDA receptors and NCX3 and stimulated oligodendrocyte differentiation [22]. Based on this observation we explored the effects of acute D-Asp treatment on calcium response in OPCs exposed to BED for 4 days + 2 days of BED washout and untreated cultures. As shown in Fig. 8, acute application of D-Asp induced a greater calcium response both in the soma and processes of immature oligodendrocytes of BED-treated, if compared to untreated cultures (Fig. 8). To explore the consequence of the augmented reversal NCX activity and calcium response on differentiation and myelin formation in oligodendrocytes, the BED-free washout was prolonged for 4 days. Analysis of oligodendrocyte morphology with phalloidin staining showed that a higher number of cells with partial or fully ring-like morphology (myelinating oligodendrocytes) was detected in cultures treated with BED for 4 days + 4 days of washout if compared to untreated cells (Fig. 9A). A punctuated distribution of NCX3 immunoreactivity was detected in the soma and along processes of MBP-stained of cells in both treated and untreated cultures (Fig. 9B). Quantitative colocalization experiments performed with anti-NCX3 and anti-MBP antibodies revealed that the percentage of MBP^+ cells coexpressing NCX3 and the quantification of MBP-stained area were significantly higher in BED-treated if compared to untreated cells (Fig. 9).

4. Discussion

The present study demonstrated that drug-free washout after a prolonged blocking of NCX3 exchanger with the pharmacological inhibitor BED enhanced NCX3 expression, stimulated reversal I_{NCX} activity, and accelerated myelin sheet formation in oligodendrocytes. Our survival and biochemical studies showed that NCX3 inhibition with the BED blocker did not significantly affected oligodendrocyte survival and NCX3 expression levels, although some increase can be detected after prolonged drug exposure (6 days). In this regard, it should be considered that the increased MTT reduction may also reflect an increased cell proliferation following BED exposure, as supported by our findings showing that BED exposure increased the number of OPCs coexpressing the nuclear proliferation marker Ki67.

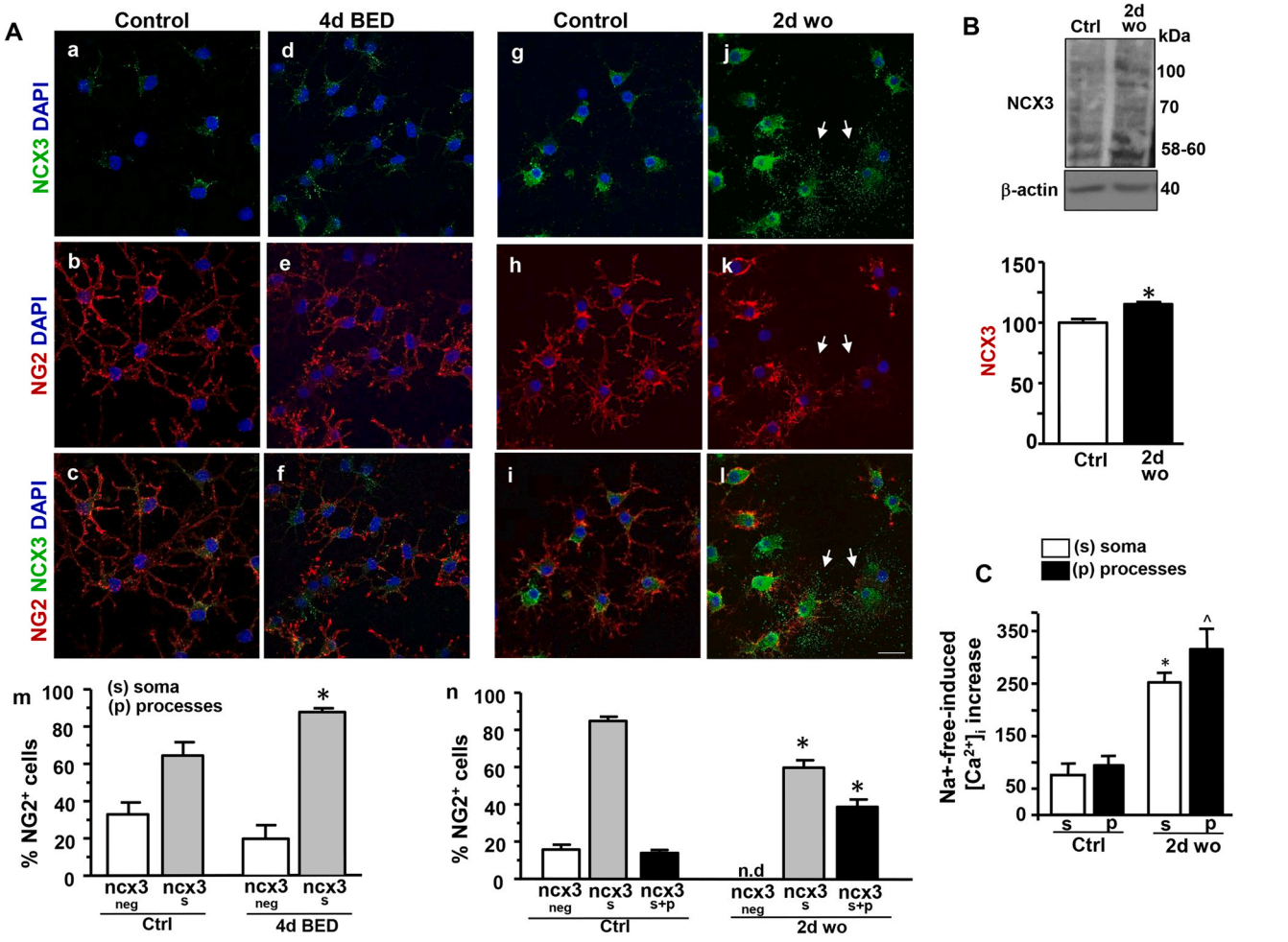

Fig. 7. Effects of 4-days BED treatment and washout on NCX3 expression and NCX activity in rat primary OPCs. A, Confocal microscopic images displaying NCX3 (green) and NG2 (red) immunoreactivities in rat primary OPCs in absence or in presence of BED for 4 days (a-c and d-f, respectively) and in OPCs under control conditions or exposed to BED treatment for 4 days + 2 days of drug-washout (g-i and j-l, respectively). Nuclei were counterstained with dapi (blue). Arrows in j-l point to multipolar $NG2^+$ cells displaying NCX3 immunosignal in soma and along cell processes. Scale bars in a-l: 20 μm. (m); quantitative analysis of the number of $NG2^{+}/NCX3^{-}$ and double-labelled $NG2^{+}/NCX3^{+}$ cells displaying NCX3 immunoreactivity in the soma (s) or along processes (p) under control conditions and 4 days after BED exposure; (n), quantitative analysis of the number of $NG2^{+}/NCX3^{-}$ and double-labelled $NG2^{+}/NCX3^{+}$ cells displaying NCX3 immunoreactivity in the soma (s) or along processes (p) under control conditions and 4 days after BED exposure + 2 days of BED-washout. Data were normalized on the total number of $NG2^+$ cells and expressed as percentage of control. The values represent the means±S.E.M. ($n = 3$). * $p < 0.05$ versus control. **B,** Western blotting and densitometric analysis of NCX3 protein levels from homogenates of rat primary OPCs under control conditions, and after 4 days of BED treatment + 2 days of drug-washout. The data were normalized on the basis of *β*-actin levels and expressed as percentage of control. The values represent the means±S.E.M. (n = 3). *p < 0.05 versus control. **C,** Quantification of NCX activity measured as Na^+-free-induced $[Ca^{2+}]_i$ increase, quantified as Δ% of peak versus basal values, in the soma (s) and processes (p) of rat primary OPCs cultured under control conditions, and after 4 days of BED treatment + 2 days of BED washout (2d wo). Each bar represents the mean±S.E.M. of the data obtained from 20 cells per group in three independent experimental sessions. *p < 0.05 versus respective control; ^p < 0.05 versus soma at 2d wo. (For interpretation of the references to colour in this figure legend, the reader is referred to the web version of this article.)

Recently, it has been pointed out that prolonged exposure to NCX blockers differentially affected intracellular $[Na^+]_i$ and $[Ca^{2+}]_i$ and, consequently, may alter cell viability [24]. Indeed, pharmacological compounds blocking the forward, but not the reverse mode of NCX, by increasing intracellular $[Ca^{2+}]_i$ are toxic to glioblastoma cells [24]. Our functional analysis showed that 4 days exposure to 100 nM BED significantly inhibited both the forward and reverse NCX operational modes and increased $[Na^+]_i$ in oligodendrocytes. We previously showed that 10–100 nM BED dose-dependently inhibited both the forward and reverse NCX3 mode of operation, moderately inhibited the reverse mode of NCX2, while failed to modulate NCX1 in BHK cell line stably transfected with each of the NCX isoforms [26]. In our MO3.13 oligodendrocyte cultures, 10 nM BED treatment failed to significantly block I_{NCX} after 4 days of treatment, possibly suggesting that the prolonged incubation time may affect the potency of BED inhibitor in oligodendrocytes.

Although further studies are needed to clarify the mechanisms underlying the $[Na^+]_i$ increase during BED exposure, it is plausible that the inhibition of both NCX3 and NCX2 exchangers activities may contribute. More interestingly, we found that drug suspension after 4 days of continuous 100 nM BED exposure promoted a significant $[Ca^{2+}]_i$ rise in oligodendrocytes, suggesting that reversal NCX activity, driven by sodium accumulation, contributed to such increase. Accordingly, several evidence demonstrated that NCX can reverse upon increase in $[Na^+]_i$ and function as a Ca^{2+} loader in brain cells under physiological and pathophysiological conditions [6,43–45]. More interestingly, we found that drug suspension after 4 or 6 days of BED exposure differentially modulated NCXs expression and NCX activity. BED-free washout after NCX3 inhibition for 6 days significantly upregulated the 58–60 kDa protein of NCX3, an effect that was accompanied by the concomitant upregulation of both NCX1 and NCX2 proteins, and increased NCX activity in the reverse and forward mode. Early data have hypothesized that, under pathophysiological conditions, calpain cleaves and

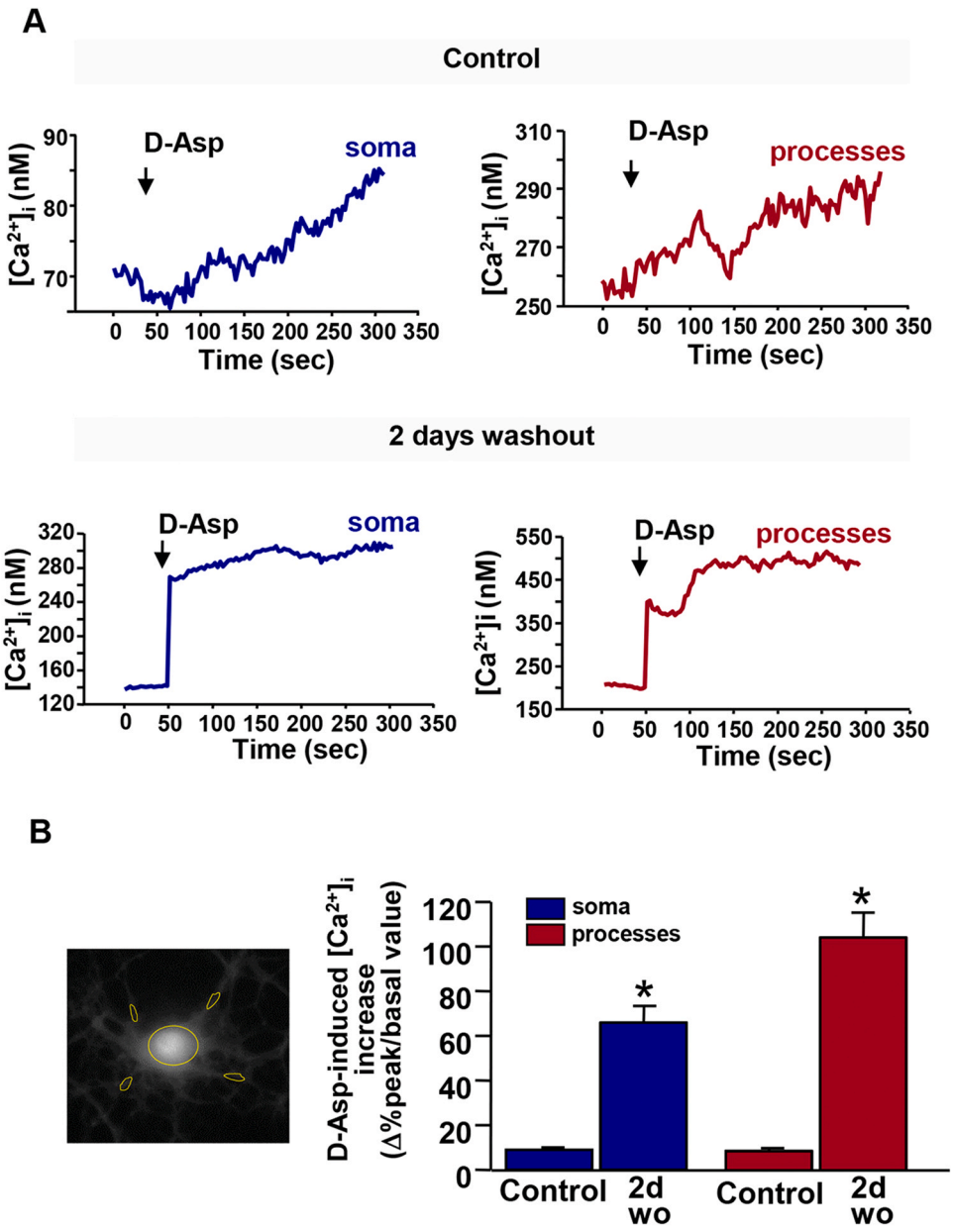

Fig. 8. D-Aspartate-induced calcium response in rat primary OPCs exposed to 4-days BED treatment + 2 days of drug-free washout. A, Superimposed single-cell traces representative of the effect of 100 μM acute D-Asp exposure on $[Ca^{2+}]_i$ detected in the soma (left panels) or processes (right panels) of rat primary OPCs under control conditions and after 4-days of BED treatment + 2 days of drug-free washout. **B,** Quantification of $[Ca^{2+}]_i$ increase showed in A, measured as Δ% of peak versus basal values. A representative cell with traced rows at the soma and proximal processes is showed on the left. Each bar represents the mean±S.E.M. of the data obtained from 10 cells per group in three independent experimental sessions. * $p < 0.05$ versus respective control.

inactivates NCX3, and this inactivation prevented the extrusion of excess neuronal Ca^{2+} contributing to Ca^{2+} dysregulation and death [39, 46–49]. This observation may suggest that NCX1 and NCX2 levels may increase in response to the proteolytic NCX3 cleavage contributing to the upregulated NCX currents recorded in oligodendrocytes during drug-free washout after 6 days of drug treatment. More intriguingly, BED-free washout after 4 days of drug treatment transiently increased NCX2 proteins at 1 day, while selectively upregulated the 70 kDa and 58–60 kDa NCX3 proteins at 2 days, an effect that was accompanied by a selective increase in reversal NCX activity. Previous findings showed that calpain-mediated NCX3 cleavage in neuronal cultures may generate the appearance of a 75 kDa and 58–60 kDa proteolytic NCX3 bands that are NCX3 hyperfunctional forms contributing to ER Ca^{2+} refilling, helping neurons to mitigate ER stress during Aβ exposure [18,50]. The calpain proteolysis of NCX3 sequence may generate three products [39] and site-directed mutagenesis showed that the removal of two lysine residues (370–371) in the consensus site for calpain cleavage in the f-loop of NCX3 sequence prevented the formation of the hyperfunctional fragment, and abolished the $A\beta_{1-42}$ stimulatory effect on NCX3 [18]. These findings, together with our results showing that *ncx3* gene silencing significantly prevented the upregulation of reversal I_{NCX}, support our hypothesis that it is NCX3 that predominantly contribute to the increased NCX reversal activity in the 4-days BED treatment protocol. On the other hand, we cannot exclude the possibility that the activity of the other two NCXs regulated the intracellular ionic changes leading to NCX3 increase. Based on our findings showing that the prolonged pharmacological inhibition of NCX3 isoform also altered the expression of the other NCXs, it is also possible that similar alterations might be observed after prolonged NCX3 gene silencing.

Moreover, $[Ca^{2+}]_i$ levels recorded after 3 h of BED washout were significantly higher than that measured after 2 days of washout, a time point in which only the NCX reverse mode significantly increased. In this regard, our biochemical studies showed that NCX2 levels were slightly and transiently upregulated one day after drug washout, indicating that, at this early time point, its activity may also contribute to $[Ca^{2+}]_i$ increase. On the other hand, due to the persistent Ca^{2+} entrance, it is also possible to hypothesize that a compensatory refilling of calcium into intracellular organelles may occur after 2 days of BED washout.

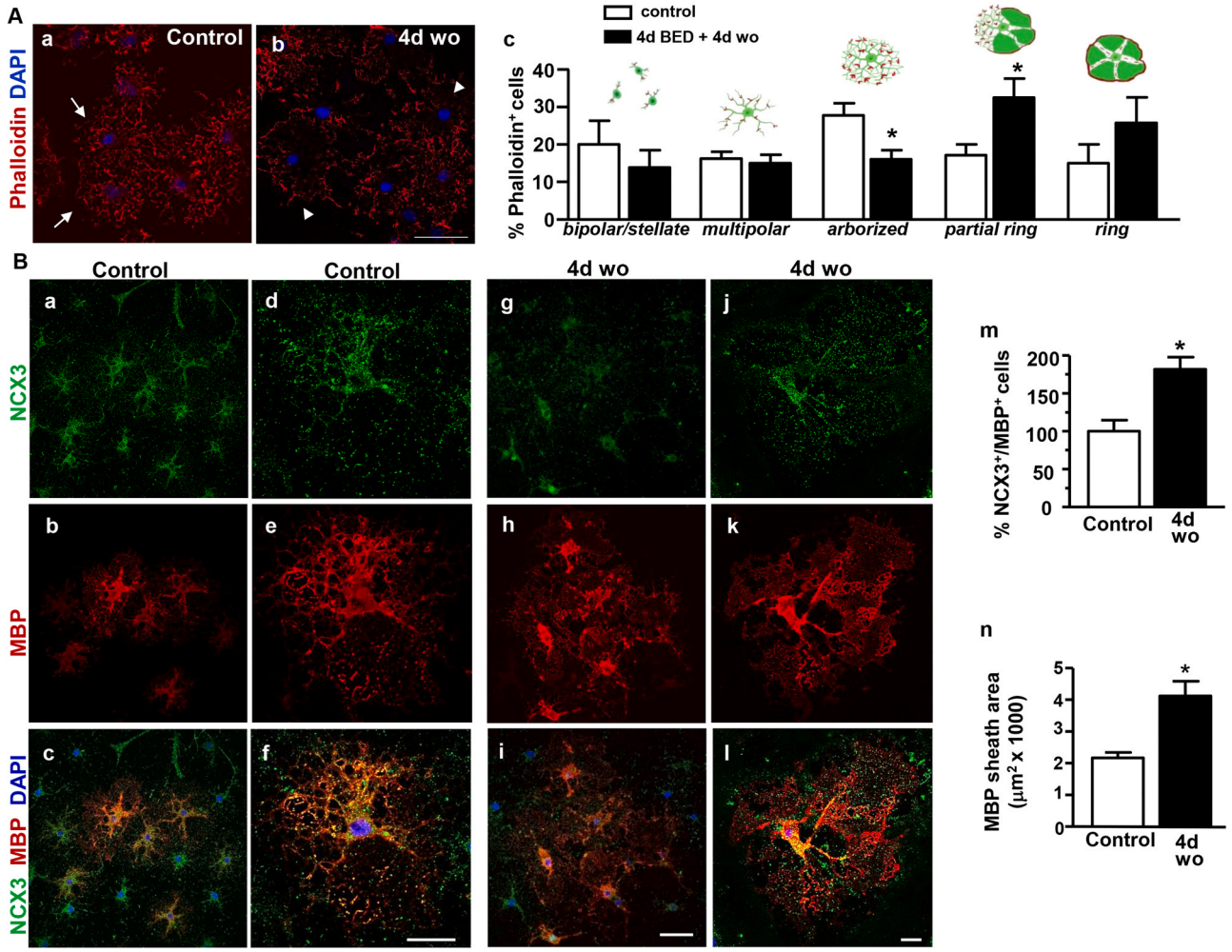

Fig. 9. Distribution of NCX3 and MBP immunoreactivities in rat primary OPCs exposed to 4-days BED treatment + 4 days of drug-free-washout. A, Representative confocal images displaying the distribution of phalloidin in OPCs under control conditions (a) or after 4-days of BED treatment + 4 days of drug-free washout (b). Arrows and arrowheads in a-b point to phalloidin-stained cells with arborized or ring morphology, respectively. Scale bars in a-b 20 μm. (c), quantitative analysis of the number of phalloidin $^{+}$ cells with bipolar/stellate, multipolar, arborized, partial ring, ring morphology. Data were normalized on the number of total number of phalloidin^{+} cells. The values represent the means±S.E.M. ($n = 3$). * $p < 0.05$ versus control. **B**, Representative confocal images displaying the distribution of NCX3 (green) and MBP (red) immunosignals in oligodendrocyte cultures under control conditions (a-f) and after 4 days of BED treatment + 4 days of drug-free-washout (g-l). Panels d-f and j-l show higher magnification images of a single representative NCX3^{+}/MBP^{+} under control conditions and after 4 days of BED treatment + 4 days of drug-free-washout, respectively. (m); quantitative analysis of the number of NCX3^{+}/MBP^{+} cells in control cultures and in cultures exposed to 4 days of BED treatment + 4 days of drug-free-washout. Data were normalized on the number of total NCX3^{+} cells and expressed as percentage of control. The values represent the means±S.E.M. ($n = 3$). * $p < 0.05$ versus control. (n), quantitative analysis of the MBP-positive area from partial ring and ring cells. Nuclei were counterstained with dapi (blue). Scale bars in a-c and g-i: 50 μm; in d-f-i: 20 μm; in j-l: 20 μm. (For interpretation of the references to colour in this figure legend, the reader is referred to the web version of this article.)

Accordingly a functional coupling between NCX3 reverse mode and ER Ca^{2+} store has been already demonstrated by our research group [18]. In this regard, although a detailed analysis of the subcellular localization of low molecular weight forms of NCX3 is lacking, our immunocytochemical studies showed that NCX3 immunoreactivity increased not only along some plasma membrane domains but also in the cytosolic compartment.

Beside the important role in delaying neuronal death, the activation of reversal NCX3 plays a more physiological function in oligodendroglia as it is required for myelin synthesis [17,20]. In fact, NCX-mediated Ca^{2+} influx sustains both spontaneous and D-Aspartate triggered $[Ca^{2+}]_i$ oscillations in differentiating oligodendrocytes and blocking NCX3 pharmacologically or silencing *ncx3* gene prevented myelin formation [7,17,21,22]. In agreement with these observations, we found that 4-days of BED treatment was associated with increased OPCs proliferation, while BED washout reduced proliferation, elevated CaMKIIβ, a critical regulator of oligodendrocyte maturation [41,51] and upregulated reversal I_{NCX} and NCX3 immunoreactivity in the soma and processes of differentiating oligodendrocytes. Recently, it has been suggested that ryanodine receptors (RyRs) and the α_2-NKA cooperate with NCXs to generate calcium transients, and a local RyRs-NCXs-α_2-NKA interaction in oligodendrocyte processes might influence myelin synthesis [52]. Interestingly, our studies showed that the 4 days, but not the 2-days BED treatment protocol significantly and transiently downregulated the α_2-NKA protein levels at 1 day of washout. The reason for this transient alteration remains to be clarified but may be linked to the rapid $[Na^{+}]_i$ and $[Ca^{2+}]_i$ changes after prolonged NCX3 blocking and drug-free washout. For instance, early data showed that the activation of the Ca^{2+}/calmodulin-dependent kinase kinase β following $[Ca^{2+}]_i$ increase has been linked to AMP-activated kinase activation and NKA endocytosis [53]. Our findings may also suggest that the low α_2-NKA expression, and possibly activity, would prime NCX for reverse mode exchange, consequently boosting oligodendrocyte development. In support of this hypothesis, and beside the

specific role for the α_2 isoform as a regulator, via NCX exchanger, of calcium and contractility in the heart [54], Hammann et al. [21] showed that knocking-down or blocking α_2-NKA activity with ouabain in oligodendrocytes increased NCX activity and anticipated the onset of MBP synthesis.

In agreement, we found that BED treatment for 4-days + 2 days of washout not only induced a significant higher calcium response in OPC soma and processes after acute D-Aspartate exposure, but also upregulated NCX3 expression along processes and accelerated oligodendrocyte maturation and myelin sheet formation. We found that Ca^{2+} concentrations were always higher in processes than in the soma, either in absence of D-Asp. This finding is in line with previous studies showing that local Ca^{2+} events within processes of differentiating oligodendrocytes modulate MBP synthesis in vitro and in vivo [1,2,52]. We previously showed that D-Asp-induced calcium responses in oligodendrocytes promotes an orchestrated activation of glutamate transporters, glutamate AMPA and NMDA receptors, and NCX3 exchangers, and drives cell differentiation [22,55]. Hence, the upregulated expression and activity of NCX3 exchanger might contribute to the different kinetics of D-Asp response under control conditions and after 2 days of BED washout. In addition, in line with the characteristic stage-specific Ca^{2+} activity of oligodendrocyte lineage, BED-treated oligodendrocytes showed a more "flat" Ca^{2+} signaling, if compared to control cultures, that displayed characteristics OPCs oscillatory pattern with peak and plateau transients [56,57].

Collectively, our findings demonstrated that the modulation of NCX3 exchanger may significantly influence intracellular $[Ca^{2+}]_i$ and $[Na^+]_i$ concentrations and related cellular processes, including myelin formation in oligodendroglia. Additionally, as a rebound activation of NCX3 exchanger may occur after the suspension of a drug that inhibits its function, particular attention should be paid to the use of NCX inhibitors in different pathophysiological conditions in which they have been proposed. Nevertheless, further studies will be necessary to understand the pharmacological effects of NCX3 inhibition in brain cells and whether the rebound activation of NCX3 following its pharmacological inhibition may represent a novel strategy to modulate NCX3 exchanger in demyelinating diseases.

Funding

This work was supported by grants from Fondazione Italiana Sclerosi Multipla FISM 2015/R/6 to F.B.; Ministry for Education, University and Research- PRIN 2017 Prot. 20175SA5JJ to F.B.

CRediT authorship contribution statement

Mariarosaria Cammarota: Data curation, Visualization, Formal analysis, Investigation. **Valeria de Rosa:** Investigation, Formal analysis. **Anna Pannaccione:** Visualization, Formal analysis, Investigation. **Agnese Secondo:** Visualization, Formal analysis, Investigation. **Valentina Tedeschi:** Investigation. **Ilaria Piccialli:** Investigation. **Ferdinando Fiorino:** Investigation. **Beatrice Severino:** Investigation. **Lucio Annunziato:** Resources. **Francesca Boscia:** Conceptualization, Data curation, Visualization, Formal analysis, Investigation, Resources, Funding acquisition, Writing the manuscript.

Conflict of interest statement

The authors report no conflict of interest.

Data Availability

Data are available on reasonable request to the corresponding author.

Appendix A. Supporting information

Supplementary data associated with this article can be found in the online version at doi:10.1016/j.biopha.2021.112111.

References

[1] A.M. Krasnow, M.C. Ford, L.E. Valdivia, S.W. Wilson, D. Attwell, Regulation of developing myelin sheath elongation by oligodendrocyte calcium transients in vivo, Nat. Neurosci. 21 (2018) 24–28, https://doi.org/10.1038/s41593-017-0031-y.

[2] M. Baraban, S. Koudelka, D.A. Lyons, Ca2+ activity signatures of myelin sheath formation and growth in vivo, Nat. Neurosci. 21 (2018) 19–23, https://doi.org/10.1038/s41593-017-0040-x.

[3] M. Papa, A. Canitano, F. Boscia, P. Castaldo, S. Sellitti, H. Porzig, M. Taglialatela, L. Annunziato, Differential expression of the Na+-Ca2+ exchanger transcripts and proteins in rat brain regions, J. Comp. Neurol. 461 (2003) 31–48, https://doi.org/10.1002/cne.10665.

[4] L. Annunziato, F. Boscia, G. Pignataro, Ionic transporter activity in astrocytes, microglia, and oligodendrocytes during brain ischemia, J. Cereb. Blood Flow Metab. 33 (2013) 969–982, https://doi.org/10.1038/jcbfm.2013.44.

[5] F. Boscia, C.D. Avanzo, A. Pannaccione, A. Secondo, A. Casamassa, L. Formisano, N. Guida, A. Scorziello, G. Di Renzo, L. Annunziato, New roles of NCX in glial cells: activation of microglia in ischemia and differentiation of oligodendrocytes, Adv. Exp. Med. Biol. 961 (2013) 307, https://doi.org/10.1007/978-1-4614-4756-6_26.

[6] F. Boscia, G. Begum, G. Pignataro, R. Sirabella, O. Cuomo, A. Casamassa, D. Sun, L. Annunziato, Glial Na(+) -dependent ion transporters in pathophysiological conditions, Glia 64 (2016) 1677–1697, https://doi.org/10.1002/glia.23030.

[7] F. Boscia, V. de Rosa, M. Cammarota, A. Secondo, A. Pannaccione, L. Annunziato, The Na+/Ca2+ exchangers in demyelinating diseases, Cell Calcium 85 (2020), 102130, https://doi.org/10.1016/j.ceca.2019.102130.

[8] P.K. Stys, S.G. Waxman, B.R. Ransom, Ionic mechanisms of anoxic injury in mammalian CNS white matter: role of Na+ channels and Na(+)-Ca2+ exchanger, J. Neurosci. 12 (1992) 430–439, https://doi.org/10.1523/jneurosci.12-02-00430.1992.

[9] P.K. Stys, R.M. Lopachin, Mechanisms of calcium and sodium fluxes in anoxic myelinated central nervous system axons, Neuroscience 82 (1998) 21–32, https://doi.org/10.1016/s0306-4522(97)00230-3.

[10] M.J. Craner, B.C. Hains, A.C. Lo, J.A. Black, S.G. Waxman, Co-localization of sodium channel Nav1.6 and the sodium-calcium exchanger at sites of axonal injury in the spinal cord in EAE, Brain 127 (2004) 294–303, https://doi.org/10.1093/brain/awh032.

[11] M.J. Craner, J. Newcombe, J.A. Black, C. Hartle, M.L. Cuzner, S.G. Waxman, Molecular changes in neurons in multiple sclerosis: altered axonal expression of Nav1.2 and Nav1.6 sodium channels and Na+/Ca2+ exchanger, Proc. Natl. Acad. Sci. U. S. A. 101 (2004) 8168–8173, https://doi.org/10.1073/pnas.0402765101.

[12] S.G. Waxman, Axonal conduction and injury in multiple sclerosis: the role of sodium channels, Nat. Rev. Neurosci. 7 (2006) 932–941, https://doi.org/10.1038/nrn2023.

[13] G. Barsukova, M.A. Forte, D. Bourdette, Focal increases of axoplasmic Ca2+, aggregation of sodium-calcium exchanger, N-type Ca2+ channel, and actin define the sites of spheroids in axons undergoing oxidative stress, J. Neurosci. 32 (2012) 12028–12037, https://doi.org/10.1523/jneurosci.0408-12.2012.

[14] A. Omelchenko, A.B. Shrirao, A.K. Bhattiprolu, J.D. Zahn, R.S. Schloss, S. Dickson, D.F. Meaney, N.N. Boustany, M.L. Yarmush, B.L. Firestein, Dynamin and reverse-mode sodium calcium exchanger blockade confers neuroprotection from diffuse axonal injury, Cell Death Dis. 27 (2019) 710–727, https://doi.org/10.1038/s41419-019-1908-3.

[15] P. Molinaro, O. Cuomo, G. Pignataro, F. Boscia, R. Sirabella, A. Pannaccione, A. Secondo, A. Scorziello, A. Adornetto, R. Gala, D. Viggiano, S. Sokolow, A. Herchuelz, S. Schurmans, G.F. Di Renzo, L. Annunziato, Targeted disruption of Na+/Ca2+ exchanger 3 (NCX3) gene leads to a worsening of ischemic brain damage, J. Neurosci. 28 (2008) 1179–1184, https://doi.org/10.1523/jneurosci.4671-07.2008.

[16] P. Molinaro, D. Viggiano, R. Nisticò, R. Sirabella, A. Secondo, F. Boscia, A. Pannaccione, A. Scorziello, B. Mehdawy, S. Sokolow, A. Herchuelz, G.F. Di Renzo, L. Annunziato, Na+-Ca2+ exchanger (NCX3) knock-out mice display an impairment in hippocampal long-term potentiation and spatial learning and memory, J. Neurosci. 31 (2011) 7312–7321, https://doi.org/10.1523/jneurosci.6296-10.2011.

[17] F. Boscia, C. D'Avanzo, A. Pannaccione, A. Secondo, A. Casamassa, L. Formisano, N. Guida, S. Sokolow, A. Herchuelz, L. Annunziato, Silencing or knocking out the Na+/Ca2+ exchanger-3 (NCX3) impairs oligodendrocyte differentiation, Cell Death Differ. 19 (2012) 562–572, https://doi.org/10.1038/cdd.2011.125.

[18] A. Pannaccione, A. Secondo, P. Molinaro, C. D'Avanzo, M. Cantile, A. Esposito, F. Boscia, A. Scorziello, R. Sirabella, S. Sokolow, A. Herchuelz, G. Di Renzo, L. Annunziato, A new concept: Aβ1-42 generates a hyperfunctional proteolytic NCX3 fragment that delays caspase-12 activation and neuronal death, J. Neurosci. 32 (2012) 10609–10617, https://doi.org/10.1523/jneurosci.6429-11.2012.

[19] Casamassa, C. La Rocca, S. Sokolow, A. Herchuelz, G. Matarese, L. Annunziato, F. Boscia, Ncx3 gene ablation impairs oligodendrocyte precursor response and increases susceptibility to experimental autoimmune encephalomyelitis, Glia 64 (2016) 1124–1137, https://doi.org/10.1002/glia.22985.

[20] M. Friess, J. Hammann, P. Unichenko, H.J. Luhmann, R. White, S. Kirischuk, Intracellular ion signaling influences myelin basic protein synthesis in oligodendrocyte precursor cells, Cell Calcium 60 (2016) 322–330, https://doi.org/10.1016/j.ceca.2016.06.009.

[21] J. Hammann, D. Bassetti, R. White, H.J. Luhmann, S. Kirischuk, α2 isoform of Na+, K+-ATPase via Na^{+},Ca^{2+} exchanger modulates myelin basic protein synthesis in oligodendrocyte lineage cells in vitro, Cell Calcium 73 (2018) 1–10, https://doi.org/10.1016/j.ceca.2018.03.003.

[22] V. de Rosa, A. Secondo, A. Pannaccione, R. Ciccone, L. Formisano, N. Guida, R. Crispino, A. Fico, R. Polishchuk, A. D'Aniello, L. Annunziato, F. Boscia, D-Aspartate treatment attenuates myelin damage and stimulates myelin repair, EMBO Mol. Med. 11 (2019), e9278, https://doi.org/10.15252/emmm.201809278.

[23] D. Marangon, E. Boda, R. Parolisi, C. Negri, C. Giorgi, F. Montarolo, S. Perga, A. Bertolotto, A. Buffo, M.P. Abbracchio, D. Lecca, In vivo silencing of miR-125a-3p promotes myelin repair in models of white matter demyelination, Glia 68 (2020) 2001–2014, https://doi.org/10.1002/glia.23819.

[24] H.J. Hu, S.S. Wang, Y.X. Wang, Y. Liu, X.M. Feng, Y. Shen, L. Zhu, H.Z. Chen, M. Song, Blockade of the forward Na+ /Ca2+ exchanger suppresses the growth of glioblastoma cells through Ca2+ -mediated cell death, Br. J. Pharm. 176 (2019) 2691–2707, https://doi.org/10.1111/bph.14692.

[25] C.R. Rose, D. Ziemens, A. Verkhratsky, On the special role of NCX in astrocytes: Translating Na^{+}-transients into intracellular Ca^{2+} signals, Cell Calcium 86 (2019), 102154, https://doi.org/10.1016/j.ceca.2019.102154.

[26] A. Secondo, G. Pignataro, P. Ambrosino, A. Pannaccione, P. Molinaro, F. Boscia, M. Cantile, O. Cuomo, A. Esposito, M.J. Sisalli, A. Scorziello, N. Guida, S. Anzilotti, F. Fiorino, B. Severino, V. Santagada, G. Caliendo, G. Di Renzo, L. Annunziato, Pharmacological characterization of the newly synthesized 5-amino-N-butyl-2-(4-ethoxyphenoxy)-benzamide hydrochloride (BED) as a potent NCX3 inhibitor that worsens anoxic injury in cortical neurons, organotypic hippocampal cultures, and ischemic brain, ACS Chem. Neurosci. 19 (2015) 1361–1370, https://doi.org/10.1021/acschemneuro.

[27] F. Esposito, F. Boscia, V. Gigantino, M. Tornincasa, A. Fusco, R. Franco, P. Chieffi, The high-mobility group A1-estrogen receptor β nuclear interaction is impaired in human esticular seminomas, J. Cell. Physiol. 227 (2012) 3749–3755, https://doi.org/10.1002/jcp.24087.

[28] F. Boscia, C. Passaro, V. Gigantino, S. Perdonà, R. Franco, G. Portella, S. Chieffi, P. Chieff, High levels of GPR30 protein in human testicular carcinoma in situ and seminomas correlate with low levels of estrogen receptor-beta and indicate a switch in estrogen responsiveness, J. Cell. Physiol. 230 (2015) 1290–1297, https://doi.org/10.1002/jcp.24864.

[29] F. Boscia, F. Ferraguti, F. Moroni, L. Annunziato, D.E. Pellegrini-Giampietro, mGlu1alpha receptors are co-expressed with CB1 receptors in a subset of interneurons in the CA1 region of organotypic hippocampal slice cultures and adult rat brain, Neuropharmacology 55 (2008) 428–439, https://doi.org/10.1016/j.neuropharm.

[30] F. Boscia, C.L. Esposito, A. Di Crisci, V. de Franciscis, L. Annunziato, L. Cerchia, GDNF selectively induces microglial activation and neuronal survival in CA1/CA3 hippocampal regions exposed to NMDA insult through Ret/ERK signalling, PLoS One 4 (2009), e6486, https://doi.org/10.1371/journal.pone.0006486.

[31] F. Boscia, L. Esposito, A. Casamassa, V. de Franciscis, L. Annunziato, L. Cerchia, The isolectin IB4 binds RET receptor tyrosine kinase in microglia, J. Neurochem. 126 (2013) 428–436, https://doi.org/10.1111/jnc.12209.

[32] J.B. Zuchero, M.M. Fu, S.A. Sloan, A. Ibrahim, A. Olson, A. Zaremba, J.C. Dugas, S. Wienbar, A.V. Caprariello, C. Kantor, D. Leonoudakis, K. Lariosa-Willingham, G. Kronenberg, K. Gertz, S.H. Soderling, R.H. Miller, B.A. Barres, CNS myelin wrapping is driven by actin disassembly, Dev. Cell 34 (2015) 152–167, https://doi.org/10.1016/j.devcel.2015.06.011.

[33] A. Secondo, R.I. Staiano, A. Scorziello, R. Sirabella, F. Boscia, A. Adornetto, V. Valsecchi, P. Molinaro, L.M. Canzoniero, G. Di Renzo, L. Annunziato, BHK cells transfected with NCX3 are more resistant to hypoxia followed by reoxygenation than those transfected with NCX1 and NCX2: Possible relationship with mitochondrial membrane potential, Cell Calcium 42 (2007) 521–535, https://doi.org/10.1016/j.ceca.2007.01.006.

[34] G. Grynkiewicz, M. Poenie, R.Y. Tsien, A new generation of Ca2+ indicators with greatly improved fluorescence properties, J. Biol. Chem. 260 (1985) 3440–3450, https://doi.org/10.1016/S0021-9258(19)83641-4.

[35] C. Diarra, S. heldon, J. Church, In situ calibration and [H+] sensitivity of the fluorescent Na+ indicator SBFI, Am. J. Physiol. Cell Physiol. 280 (2001) 1623–1633, https://doi.org/10.1152/ajpcell.2001.280.6.C1623.

[36] Pannaccione, F. Boscia, A. Scorziello, A. Adornetto, P. Castaldo, R. Sirabella, M. Taglialatela, G. Di Renzo, L. Annunziato, Up-regulation and increased activity of KV3.4 channels and their accessory subunit MinK-related peptide 2 induced by amyloid peptide are involved in apoptotic neuronal death, Mol. Pharm. 72 (2007) 665–673, https://doi.org/10.1124/mol.107.034868.

[37] F. Boscia, A. Pannaccione, R. Ciccone, A. Casamassa, C. Franco, I. Piccialli, V. de Rosa, A. Vinciguerra, G. Di Renzo, L. Annunziato, The expression and activity of K_V3.4 channel subunits are precociously upregulated in astrocytes exposed to Aβ oligomers and in astrocytes of Alzheimer's disease Tg2576 mice, Neurobiol. Aging 54 (2017) 187–198, https://doi.org/10.1016/j.neurobiolaging.2017.03.008.

[38] T. Iwamoto, S. Kita, YM-244769, a novel Na+/Ca2+ exchange inhibitor that preferentially inhibits NCX3, efficiently protects against hypoxia/reoxygenation-induced SH-SY5Y neuronal cell damage, Mol. Pharm. 70 (2006) 2075–2083, https://doi.org/10.1124/mol.106.028464.

[39] D. Bano, K.W. Young, C.J. Guerin, R. Lefeuvre, N.J. Rothwell, L. Naldini, R. Rizzuto, E. Carafoli, P. Nicotera, Cleavage of the plasma membrane Na+/Ca2+ exchanger in excitotoxicity, Cell 28 (2005) 275–285, https://doi.org/10.1016/j.cell.2004.11.049.

[40] F. Swift, N. Tovsrud, I. Sjaastad, O.M. Sejersted, E. Niggli, M. Egger, Functional coupling of alpha(2)-isoform Na(+)/K(+)-ATPase and Ca(2+) extrusion through the Na(+)/Ca(2+)-exchanger in cardiomyocytes, Cell Calcium 48 (2010) 54–60, https://doi.org/10.1016/j.ceca.2010.06.006.

[41] C.T. Waggener, J.L. Dupree, Y. Elgersma, B. Fuss, CaMKIIβ regulates oligodendrocyte maturation and CNS myelination, J. Neurosci. 33 (2013) 10453–10458, https://doi.org/10.1523/j.neurosci.5875-12.2013.

[42] T. Quintela-López, C. Ortiz-Sanz, M.P. Serrano-Regal, Aβ oligomers promote oligodendrocyte differentiation and maturation via integrin β1 and Fyn kinase signaling, Cell Death Dis. 10 (2019) 445, https://doi.org/10.1038/s41419-019-1636-8.

[43] S. Kirischuk, H. Kettenmann, A. Verkhratsky, Na+/Ca2+ exchanger modulates kainate-triggered Ca2+ signaling in Bergmann glial cells in situ, FASEB J. 11 (1997) 566–572, https://doi.org/10.1096/fasebj.11.7.9212080.

[44] C.L. Floyd, F.A. Gorin, B.G. Lyeth, Mechanical strain injury increases intracellular sodium and reverses Na+/Ca2+ exchange in cortical astrocytes, Glia 51 (2005) 35–46, https://doi.org/10.1002/glia.20183.

[45] N.J. Gerkau, R. Lerchundi, J.S.E. Nelson, M. Lantermann, J. Meyer, J. Hirrlinger, C. R. Rose, Relation between activity-induced intracellular sodium transients and ATP dynamics in mouse hippocampal neurons, J. Physiol. 597 (2019) 5687–5705, https://doi.org/10.1113/JP278658.

[46] D. Bano, P. Nicotera, Ca^{2+} signals and neuronal death in brain ischemia, Stroke 38 (2007) 674–676, https://doi.org/10.1161/01.str.0000256294.46009.29.

[47] I.M. Araújo, B.P. Carreira, T. Pereira, P.F. Santos, D. Soulet, A. Inácio, B.A. Bahr, A. P. Carvalho, A.F. Ambrósio, C.M. Carvalho, Changes in calcium dynamics following the reversal of the sodium-calcium exchanger have a key role in AMPA receptor-mediated neurodegeneration via calpain activation in hippocampal neurons, Cell Death Differ. 14 (2007) 1635–1646, https://doi.org/10.1038/sj.cdd.4402171.

[48] T. Brustovetsky, A. Bolshakov, N. Brustovetsky, Calpain activation and Na+/Ca2+ exchanger degradation occur downstream of calcium deregulation in hippocampal neurons exposed to excitotoxic glutamate, J. Neurosci. Res. 88 (2010) 1317–1328, https://doi.org/10.1002/jnr.22295.

[49] J. Atherton, K. Kurbatskaya, M. Bondulich, C.L. Croft, C.J. Garwood, R. Chhabra, S. Wray, A. Jeromin, D.P. Hanger, W. Noble, Calpain cleavage and inactivation of the sodium calcium exchanger-3 occur downstream of Aβ in Alzheimer's disease, Aging Cell 13 (2014) 49–59, https://doi.org/10.1111/acel.12148.

[50] A. Verkhratsky, E.C. Toescu, Endoplasmic reticulum Ca(2+) homeostasis and neuronal death, J. Cell. Mol. Med. 7 (2003) 351–361, https://doi.org/10.1111/j.1582-4934.2003.tb00238.x.

[51] Z. Martinez-Lozada, C.T. Waggener, K. Kim, S. Zou, P.E. Knapp, Y. Hayashi, A. Ortega, B. Fuss, Activation of sodium-dependent glutamate transporters regulates the morphological aspects of oligodendrocyte maturation via signaling through calcium/calmodulin-dependent kinase IIβ's actin-binding/-stabilizing domain, Glia 62 (2014) 1543–1558, https://doi.org/10.1002/glia.22699.

[52] D. Bassetti, J. Hammann, H.J. Luhmann, R. White, S. Kirischuk, Ryanodine receptor- and sodium-calcium exchanger-mediated spontaneous calcium activity in immature oligodendrocytes in cultures, Neurosci. Lett. 27 (2020) 732, https://doi.org/10.1016/j.neulet.2020.134913 (134913).

[53] G.A. Gusarova, H.E. Trejo, L.A. Dada, A. Briva, L.C. Welch, R.B. Hamanaka, G. M. Mutlu, N.S. Chandel, M. Prakriya, J.I. Sznajder, Hypoxia leads to Na, K-ATPase downregulation via Ca(2+) release-activated Ca(2+) channels and AMPK activation, Mol. Cell Biol. 31 (2011) 3546–3556, https://doi.org/10.1128/MCB.05114-11 (Epub 2011 Jul 5. PMID: 21730292; PMCID: PMC3165547).

[54] F. Swift, J.A.K. Birkeland, N. Tovsrud, U.H. Enger, J.M. Aronsen, E.L. William, I. Sjaastad, O.M. Sejersted, Altered Na+/Ca2+-exchanger activity due to downregulation of Na+/K+-ATPase alpha2-isoform in heart failure, Cardiovasc Res 78 (2008) 71–78, https://doi.org/10.1093/cvr/cvn013.Epub2008Jan17.

[55] H.O. Gautier, K.A. Evans, K. Volbracht, R. James, S. Sitnikov, I. Lundgaard, F. James, C. Lao-Peregrin, R. Reynolds, R.J. Franklin, R.T. Káradóttir, Neuronal activity regulates remyelination via glutamate signalling to oligodendrocyte progenitors, Nat. Commun. 6 (2015) 6–8518, https://doi.org/10.1038/ncomms9518 (PMID: 26439639; PMCID: PMC4600759).

[56] J. Niu, T. Li, C. Yi, N. Huang, A. Koulakoff, C. Weng, C. Li, C.J. Zhao, C. Giaume, L. Xiao, Connexin-based channels contribute to metabolic pathways in the oligodendroglial lineage, J. Cell Sci. 129 (2016) 1902–1914, https://doi.org/10.1242/jcs.178731.

[57] T. Li, L. Wang, T. Ma, S. Wang, J. Niu, H. Li, L. Xiao, Dynamic calcium release from endoplasmic reticulum mediated by Ryanodine Receptor 3 is crucial for oligodendroglial. Differentiation, Front. Mol. Neurosci. 11 (2018) 162, https://doi.org/10.3389/fnmol.2018.00162.